

June 11, 1981

MUON PRODUCTION IN A TEVATRON BEAM DUMP

D.A. Garelick, M.J. Glaubman, E.L. Pothier

Northeastern University

George Glass

Northeastern University and Texas A & M University

Shu-Rong Han

Northeastern University and
The Institute of High Energy Physics, Peking

Harald Johnstad

Fermilab

Spokesperson:

Michael J. Glaubman
Northeastern University
Boston, Massachusetts 02115
Telephone: (617)437-2933/2902

TABLE OF CONTENTS

A. Introduction	p. 1
B. Summary of Physics Objectives	
I. Drell Yan, gluons and QCD	p. 1
II. Weak-electromagnetic interference	p. 2
III. Multi-muon studies	p. 3
C. The P-645 Apparatus	p. 3
D. The Data	
I. General Comments	p. 8
II. Rates	
Example 1: The asymmetry (electroweak interference) measurement	p. 8
Example 2: Angular distributions at high pperp	p. 12
E. Costs	p. 12
Appendix	p. 13

A. Introduction

In April 1980 we proposed that the beam dump contemplated for the neutrino area be built as an instrumented beam dump for dimuon physics. The proposal, P-645, was presented at the PAC meeting that April and an addendum with more detail and a reconfigured experimental arrangement was submitted to the PAC in June 1980. At that time we requested the PAC to consider the alternative of running P-645 as a stand alone experiment in a primary or secondary beam. The proposal was rejected as a neutrino associated experiment and was not considered otherwise. In January 1981 we requested the PAC to reconsider P-645 as a stand alone experiment; we have been advised that to avoid confusion we should rewrite our proposal without reference to the neutrino beam dump. This document should be interpreted as a letter of intent based on our experience on E-439 and our earlier proposals as reflected in the physics and design of P-645.

B. Summary of Physics Objectives

I) Drell Yan, gluons and QCD. Dimuon production is a sensitive and reliable tool for the study of parton (quark, antiquark, gluon) structure functions and QCD. The dimuon experiments at Fermilab have been each optimized for different purposes---high sensitivity with high resolution but poor angular and x_F acceptance, good resolution and angular and x_F acceptance but poor sensitivity, high p_{\perp} and mass sensitivity but poor polar angle and x_F acceptance, high mass sensitivity and x_F acceptance but poor resolution and angular acceptance, etc. For the Tevatron era only one dimuon experiment has been approved: E-605. Other groups have

indicated their intent to continue their dimuon physics studies as before since any dimuon physics that one can do with beams from a 400 GeV machine can be done better and easier with beams from a 1000 GeV machine.

We propose that the whole range of dimuon physics that will not be covered (properly) by E-605 should be done on one device with very high acceptance in all kinematic variables and very high sensitivity. Furthermore, the device should be highly sensitive as we go to the kinematic limit of the different variables simultaneously. We expect the measurements of dimuon production over the full kinematic range to restrict the prescriptions of QCD to the point where the theory loses its flexibility and is proven either true or false. We consider as even more interesting the possibility of discovering a completely new effect or phenomenon if the sensitivity and kinematics are taken to the extreme.

II) Weak-electromagnetic interference. Quark-antiquark annihilation to a massive dimuon state can be due to their electromagnetic charge or their weak charge, i.e., it can proceed via a γ or a Z_0 . The mass of the Z_0 is apparently much higher than the dimuon masses available even with Tevatron beams, so production via the Z_0 is too far off the resonance curve to compete with the Drell Yan process, but the interference between the γ amplitude and the Z_0 one leads to a small, but detectable, forward-backward asymmetry in the dimuon polar angle distribution. The asymmetry parameter a is the coefficient of $\cos \theta^*$, where θ^* is the angle between the outgoing μ^- and the incoming quark (not \bar{q}). Detailed descriptions of

the theory of the asymmetry measurements are given in the P-583 proposal and associated documents that were submitted to the PAC together with P-645. The experiment should be run with proton, π^- and π^+ beams of the highest intensity and energy. For high mass dimuon production, $M^2 = x_1 x_2 S > 100 \text{ GeV}^2$, the leading beam quark (x_1) and target quark (x_2) will be: for proton beam (with $x_1 - x_2 = x_F > 0.3$) $x_1 = u$, $x_2 = \bar{u}$; for π^- , $x_1 = \bar{u}$, $x_2 = u$; for π^+ , $x_1 = \bar{d}$, $x_2 = d$. The ratio of the interference term to the E.M. term will be proportional to the ratio of the weak charge to the electric charge. The asymmetry will have the same sign for the π^- and the proton (but the direction of the quark is the direction of the target for π 's) and the opposite sign for the π^+ . The fact that the secondary beams have lower intensities and energies than the primary beam is compensated for by their higher cross section. Asymmetries due to higher order electromagnetic effects can also be separated out better if all three asymmetries are measured; in any case, they hardly depend on M^2 whereas the $Z_0 - \gamma$ interference is proportional to M^2 . There are many systematic physics checks on the asymmetry measurement---for protons it should go to zero at $x_F = 0$, and in all cases the T data should (probably!) show no asymmetry.

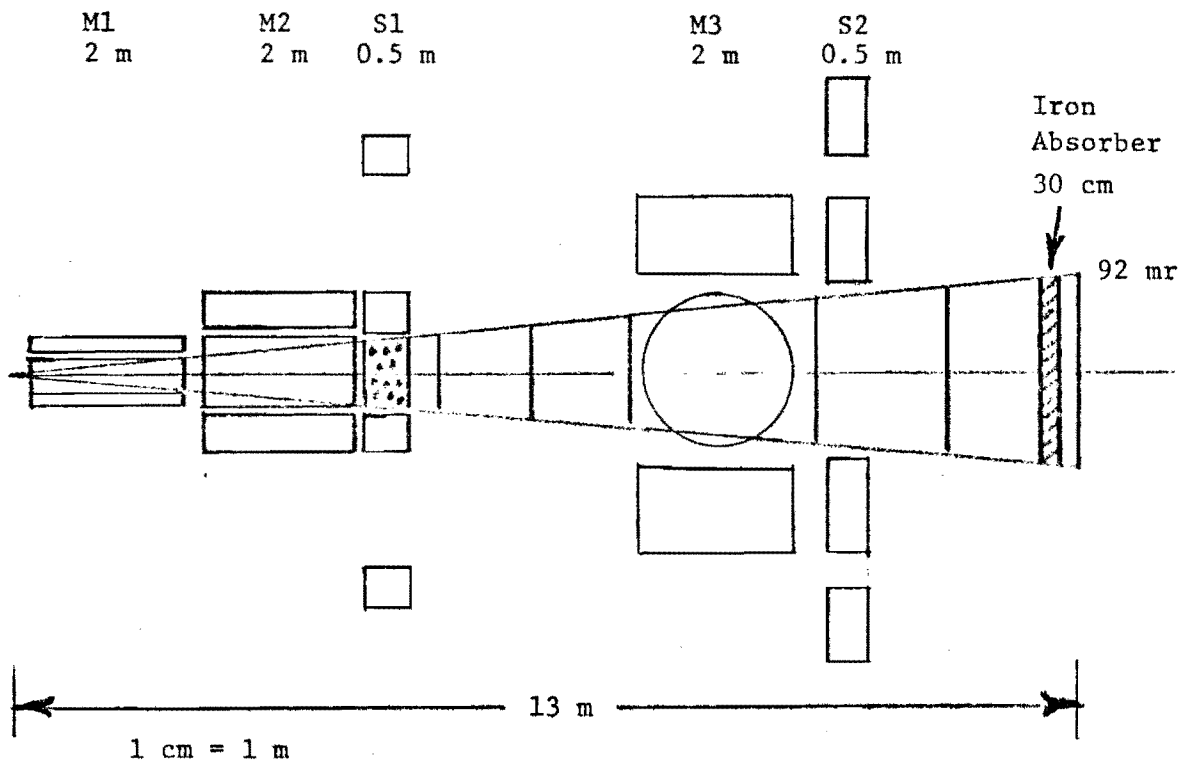
III) Multi-muon studies. The apparatus can collect excellent data on multi- states especially those that decay to $\psi\psi$ [$(\psi)^2 \rightarrow (\mu^+)^2(\mu^-)^2$, 1/2 % branching ratio].

C. The P-645 Apparatus

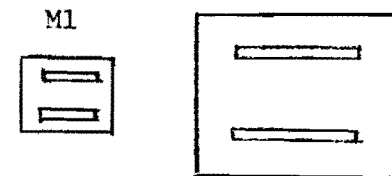
Figure I is a sketch of the apparatus. The target is followed by magnetized iron to reduce the hadronic background and to bend out (in the vertical plane) the low pperp single muons. This is followed by

Figure I

VERTICAL BEND PLANE

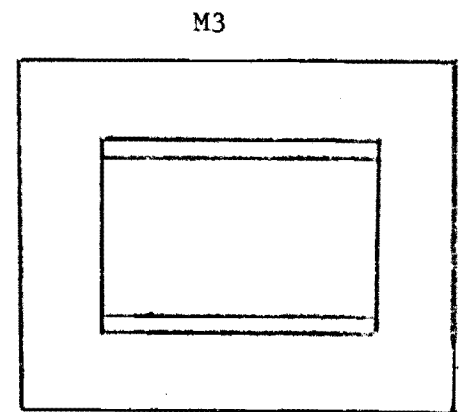


MAGNETIZED IRON

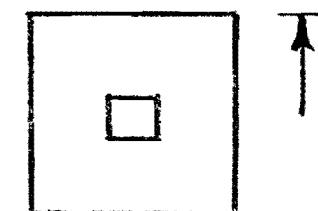
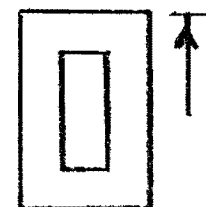
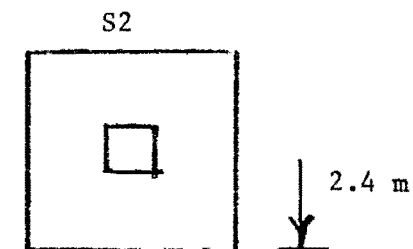
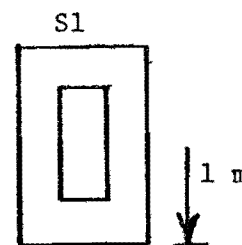


Magnet End Views

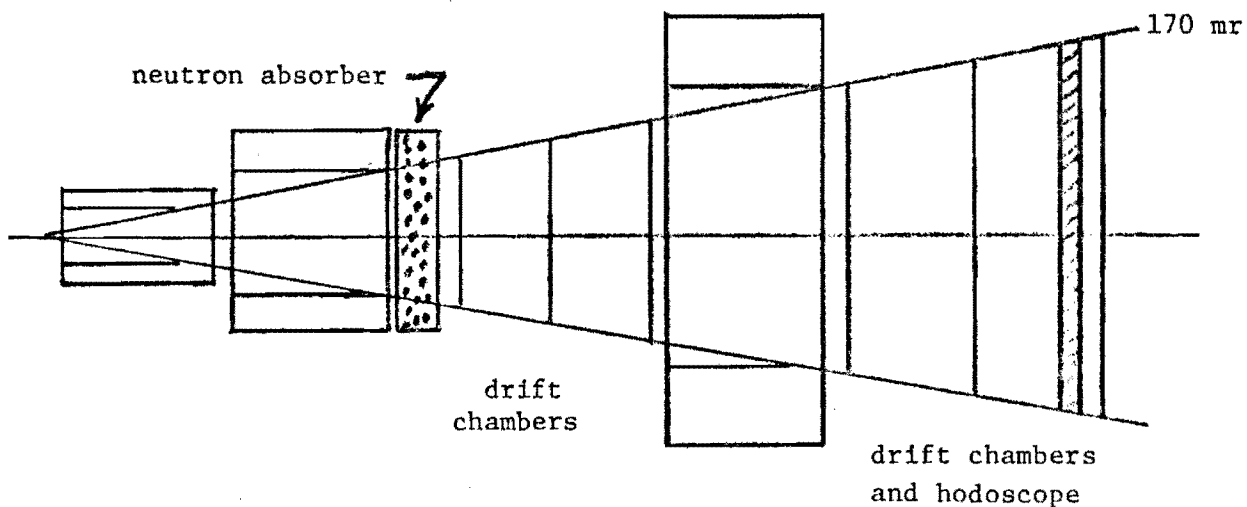
SUPER-CONDUCTING SOLENOID



SPOILERS



neutron absorber



MID HORIZONTAL (NON BEND) PLANE

a large volume superconducting solenoid for momentum analysis (also bending in the vertical plane). There are three sets of drift chambers on either side of the solenoid and three sets of hodoscopes. Each set of hodoscopes consists of an x and a y array of counters and each set of chambers consists of two x,y arrays (to remove the left right ambiguity) and a tilt. The hodoscope is used for triggering and road definition (for tracking). All the detectors have an inactive area in the shape of an X (upper and lower triangles = inactive area). The slope of the detector's inner edges is determined by P_T^S/K , where P_T^S = minimal P_T that the single μ must have to be detected, and K is the momentum kick of the magnet. There are spoilers and neutron absorbers to reduce the background in the detectors. The drawing and the numbers to be quoted below are for 800 GeV protons (4m magnetized iron) at the highest Tevatron intensities ($\sim 3 \times 10^{11}$ protons/second). Secondary beams at lower energies and intensities will be run with a smaller length of magnetized iron so as to keep the same mass and pperp resolution as for 800 GeV protons.

The momentum resolution is about 2%; the number of radiation lengths is about 300 (not involved in the momentum resolution). The $2\mu P_T$ resolution is 0.3 GeV. The mass resolution drops from 4% at 6 GeV to 3% at 9 GeV and 2% at 15 GeV and does not depend on x_F and P_T .

The singles rate in the detector depends strongly on the P_T^S cut (i.e., the slope of the wedge or X). Figure II shows the number of singles over the whole detector (62 milliradians) per μ sec. The change in the singles rate as a function of P_T^S is very large and indicates the concentration of low mass events along the X boundary. Figures IIIa and IIIb show

FIGURE II

Counts/ μ second

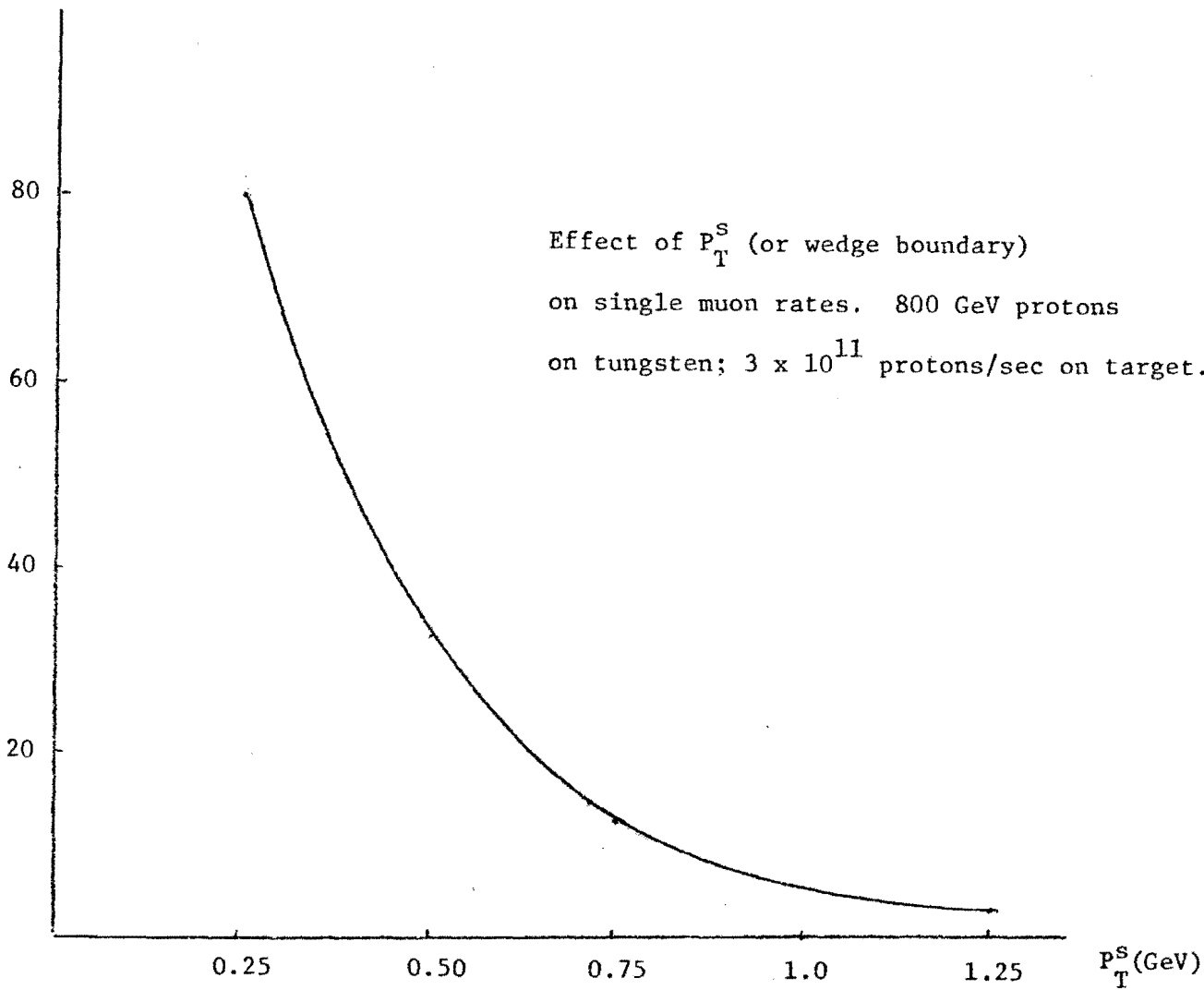
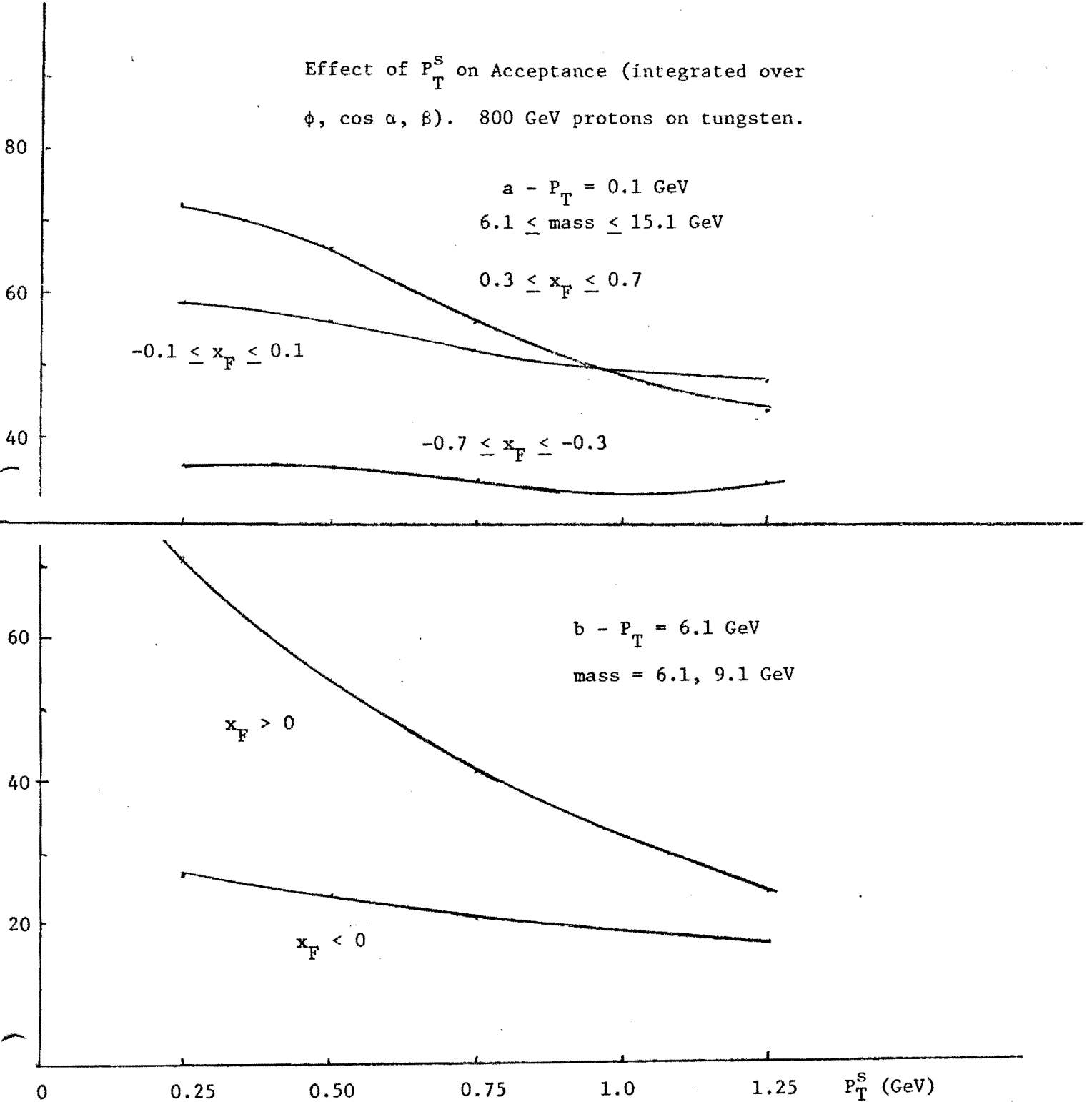


FIGURE III

Percent

Effect of P_T^S on Acceptance (integrated over ϕ , $\cos \alpha$, β). 800 GeV protons on tungsten.



the effect of P_T^S on the acceptance at low P_T and $P_T = 6$ GeV respectively.

As in E-439, matrix logic will be used to give preference to high mass or high pperp triggers. Approximately 60% of our high-mass matrix-logic triggers in E-439, which was run at comparable intensities, were two track events. Figure IV is a typical CHANCE/TRUE = (LIKE SIGN)/(UNLIKE SIGN - LIKE SIGN) vs. intensity curve from E-439. It shows how clear the dimuon signal is. Figure V shows how sharply the residual like sign fraction drops with dimuon mass (i.e., with the P_T of the muons).

D. The Data

I) General comments.

1. Very large solid angle in the dimuon center of mass system means a large lever arm for angular distribution and asymmetry measurements. This is very important for the study of the Drell-Yan process, studies of the angular and azimuthal distributions at high pperp and electroweak interference.

2. High acceptances means more events per proton on target. Protons on target will be a scarce commodity in the Tevatron era, and the people in charge should see to it that they are used most efficiently.

3. High sensitivity means that rare phenomena can be observed. Furthermore, since these may tend to be at the kinematic limits, there is a special advantage to combining wide range with high sensitivity. We have appended to this proposal a large set of geometric acceptances curves to illustrate the kinematic range we propose to cover.

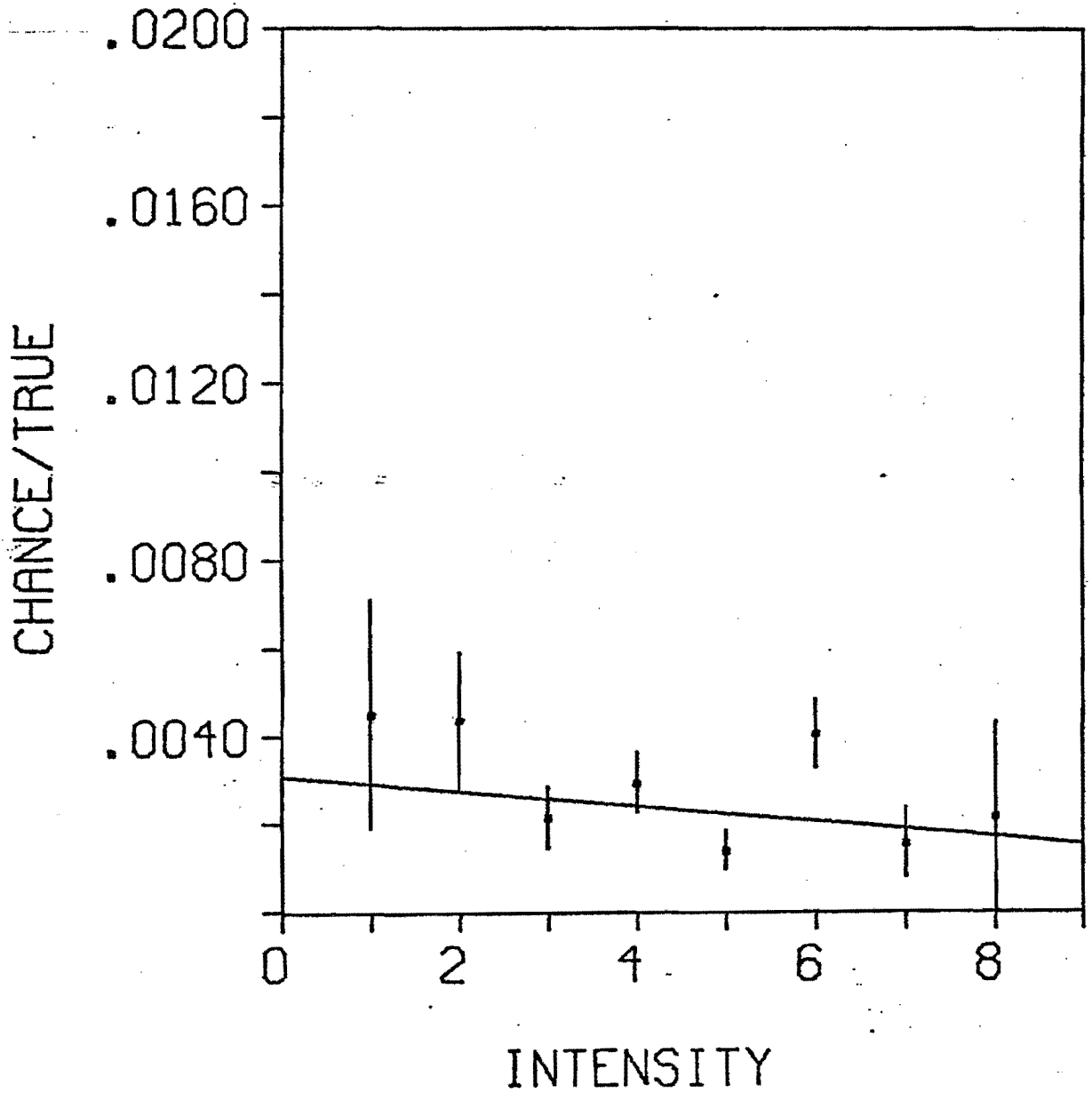
II) Rates.

Example 1: The asymmetry (electroweak interference) measurement,

Using (for 800 GeV protons)

FIGURE IV

MASS=8-9GEV



RESIDUAL VALUES (INTENSITY $\rightarrow 0$) OF
(LIKE SIGN) / (UNLIKE SIGN - LIKE SIGN)

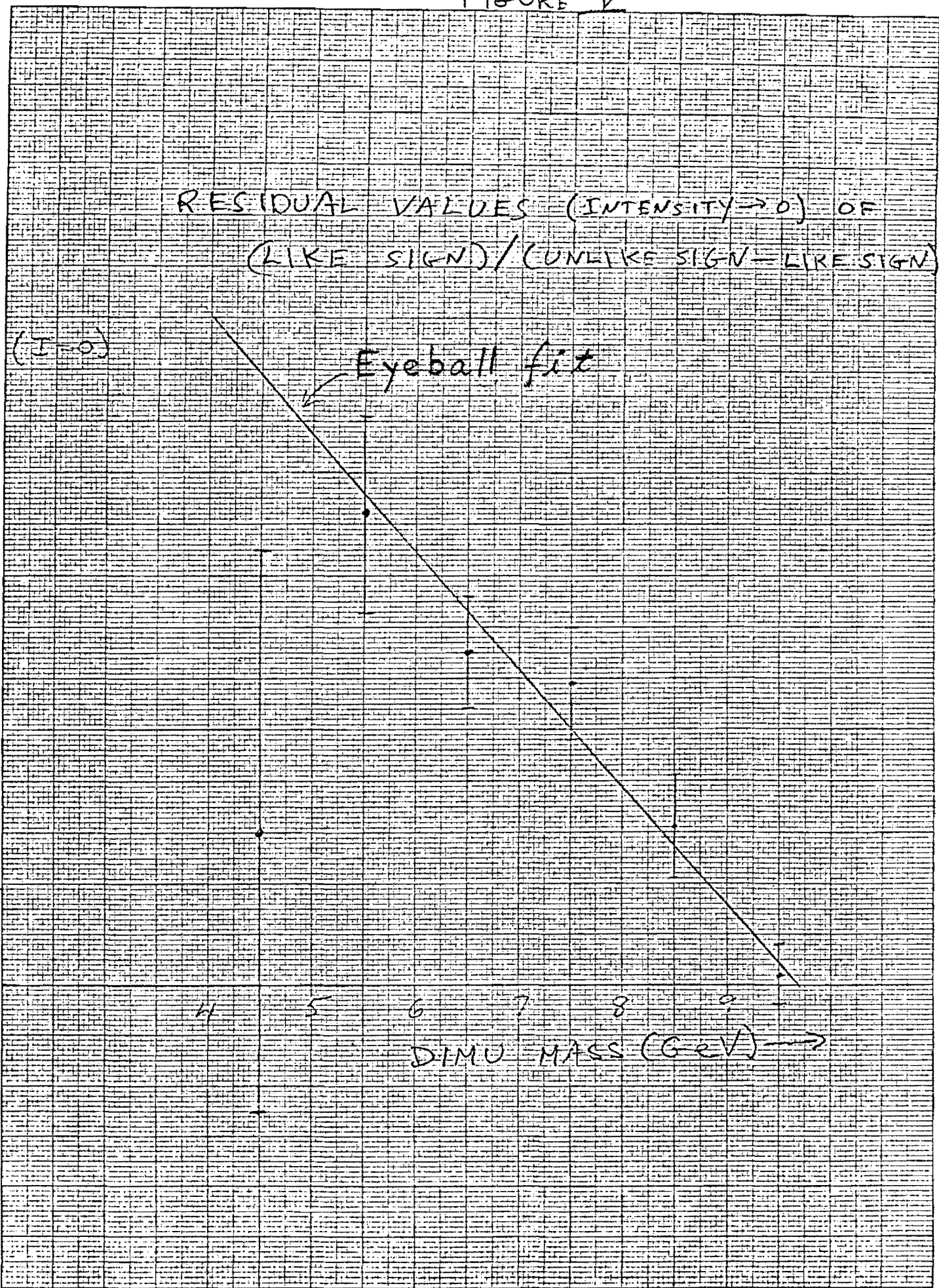
C/T (I-0)
↑
.01

↙ Eyeball fit

.005
.004
.003
.002
.001
0

4 5 6 7 8 9
DIMU MASS (GeV) \rightarrow

K&E 10 X 10 TO THE CENTIMETER 46 1510
10 X 25 CM. MADE IN U.S.A.
KEUFFEL & ESSER CO.



$$\frac{d\sigma}{dM} = 0.8 e^{-0.65M} \text{ nb/GeV}$$

and allow for an $A^{1/3}$ gain in the ratio of the Drell-Yan to total cross section (~ 40 mb) the number of dimuons at 12 GeV in a one GeV bin, per proton, is

$$\left(\frac{dN}{dM} \right)_{M=12 \text{ GeV}} = \text{Acceptance} \times 4.3 \times 10^{-11} / \text{GeV proton}$$

which translates into

$$\left(\frac{dN}{dM} \right)_{M=12 \text{ GeV}} = \text{Acceptance} \times 5 \times 10^{-12} / \text{GeV proton}$$

$$0.3 < x_F < 0.7$$

For this mass and x_F bin the acceptance is 66% for $-0.65 \leq \cos \alpha \leq 0.65$ and drops to 36% at $\cos \alpha = \pm 0.85$. Ignoring the effect of the $1+z^2$ term ($z = \cos \alpha$)

$$N^{\pm} = \int_0^{z_1} C [1 \pm az] dz = Cz_1 [1 \pm \frac{1}{2} a z_1] = \frac{1}{2} N [1 \pm \frac{1}{2} a z_1]$$

$$A = \frac{N^+ - N^-}{N} = [a z_1] / 2$$

$$A = 1/\sqrt{N} = [z_1 \delta a] / 2$$

Using Acceptance = 0.6 for $-0.8 < z < 0.8$ ($z_1 = 0.8$),

$$N = 3 \times 10^{-12} / \text{GeV proton}$$

and in 1000 hours of running at 2×10^{14} protons/hour we would have for a 1 MeV bin at 12 GeV, $0.3 \leq x_F \leq 0.7$, $N = 6 \times 10^5$ dimuons and $\delta a = 3 \times 10^{-3} \sim \frac{1}{4} a_{\gamma Z_0}$ where $a_{\gamma Z_0}$ is the contribution of γZ_0 interference to the asymmetry.

At lower mass the statistical accuracy will be higher but $a_{\gamma Z_0}$ will be a smaller part of the asymmetry; at higher mass δa will increase but $a_{\gamma Z}$

will be a more significant part of the asymmetry. We expect a reasonable measure of the interference in 1000 hours at 2×10^{14} protons/hour, and a comparable result for π beams.

Example 2: Angular distributions at high pperp.

We use

$$\frac{d^2\sigma}{dM dP_T} = 1.4 P_T e^{-0.65M-1.37 P_T} \text{ nb/GeV}^2$$

For a 1000hour run (2×10^{11} protons)

$$\left(\frac{d^2N}{dM dP_T} \right)_{\substack{M=6 \text{ GeV} \\ P_T=6 \text{ GeV}}} = \text{Acceptance} \times 10^6 \text{ events/GeV}^2$$

Considering our large average acceptance the feasibility of measuring both the angular distribution ($\cos^2 \alpha$) and the azimuthal distribution ($\cos 2\beta$) are excellent. Again we have many systematic checks---for example, the origin of β rotates throughout the apparatus, and we also have a four fold symmetry in β . For details of the acceptance in β and $\cos \alpha$ see the Appendix.

E. Costs

We estimate the magnets at \sim \$1000 K, the hodoscopes at \$150 K, the drift chambers at \$150 K and the electronics at \$500 K.

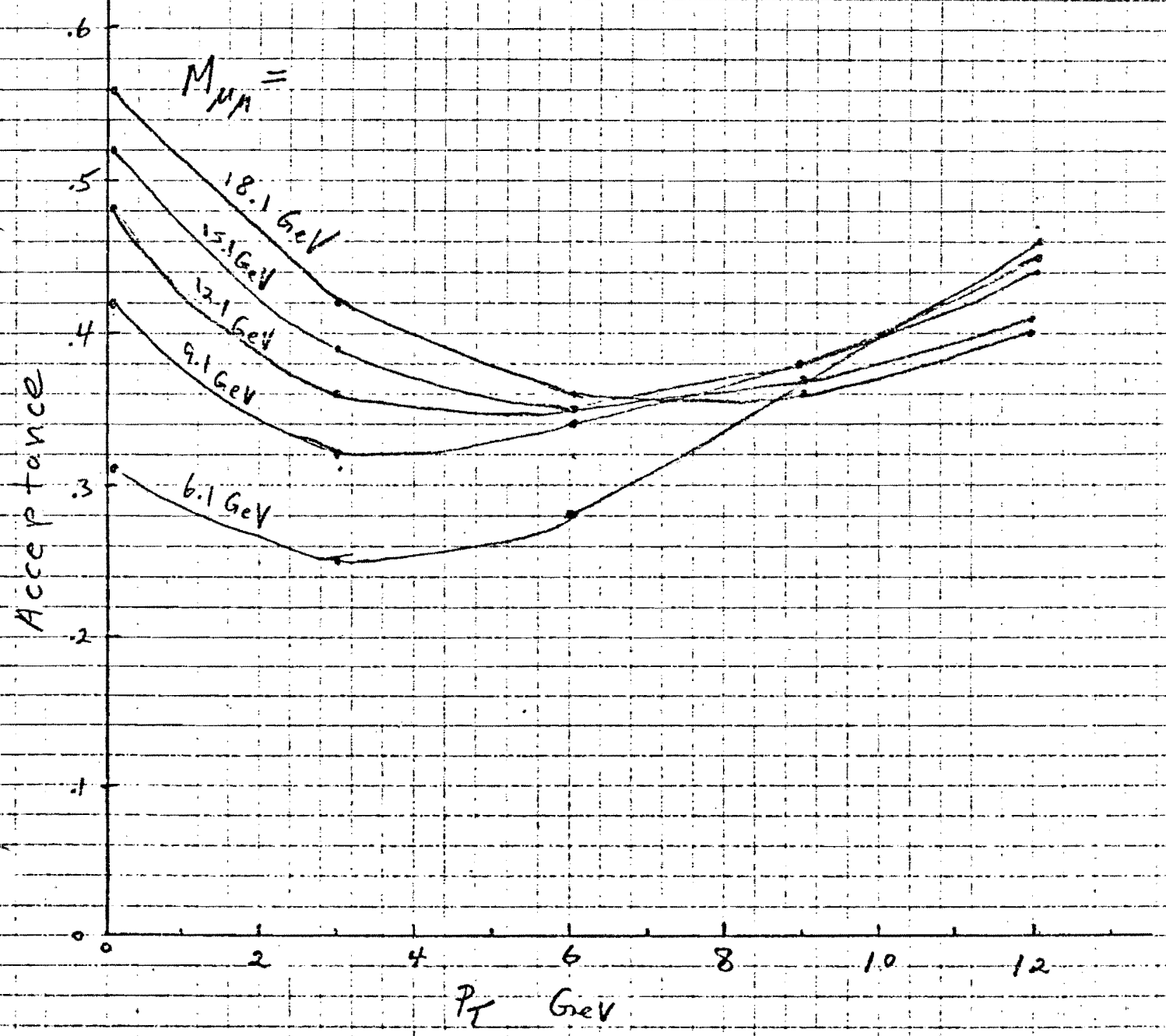
- Fig A1 -

Acceptance

$\sqrt{s} = 38.7 \text{ GeV}$

P_T dependence for different $M_{\mu\mu}$

$P_T^S = .75 \text{ GeV}$



PROTONS

ANGULAR ACCEPTANCES AT HIGH P_T ($x_F < 0$)

Fig A2
Acceptance

$M = 6.1$ and 9.1 GeV, $\sqrt{s} = 38.7$ GeV
 $x_F < 0$; $P_T = 6.1$ GeV

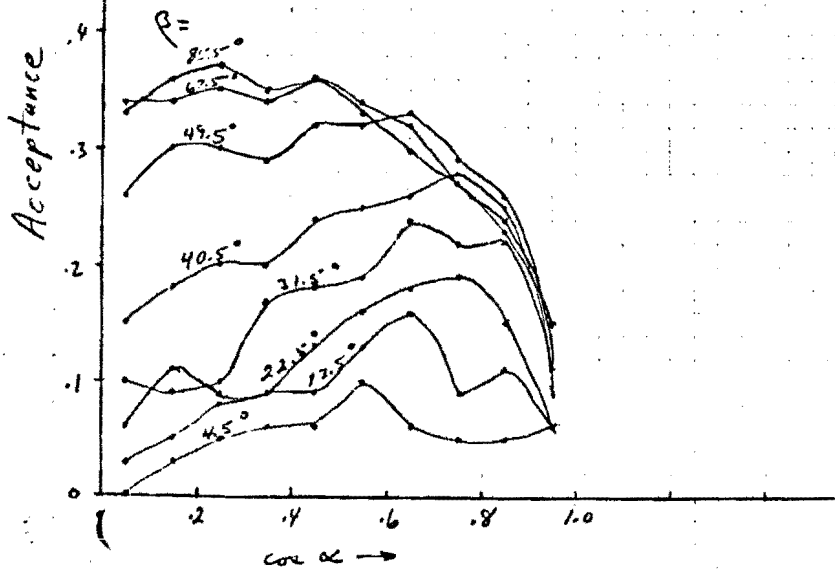
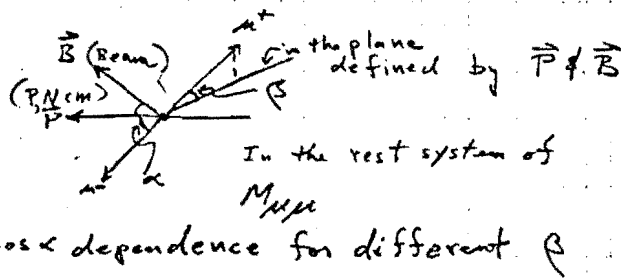
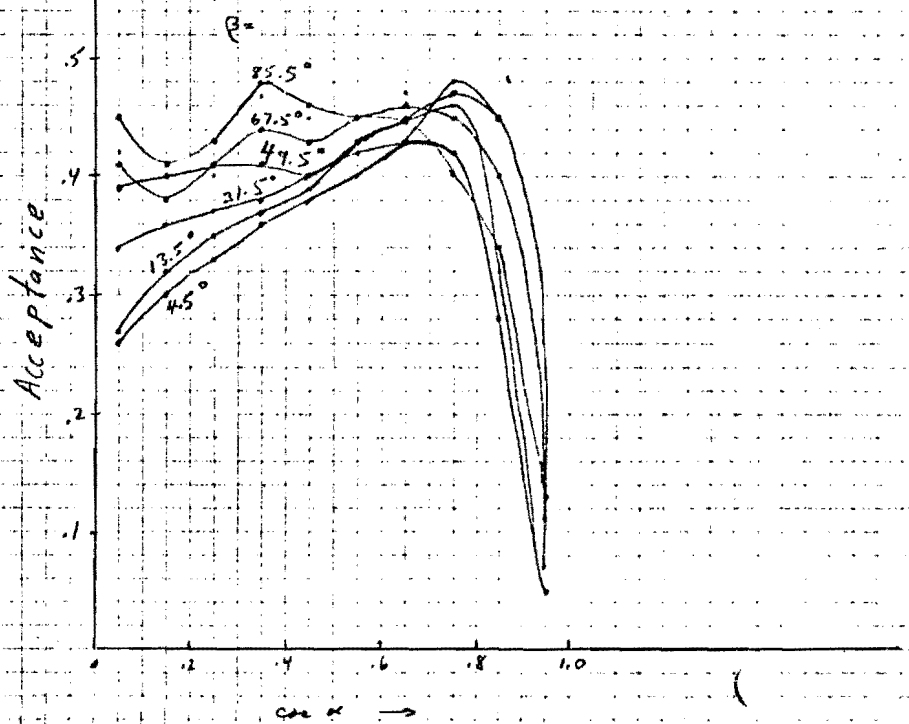


Fig. A3
Acceptance

$M = 6.1$ and 9.1 GeV, $\sqrt{s} = 38.7$ GeV
 $x_F < 0$, $P_T = 12.1$ GeV
Cos α dependence for different β



-14-

PROTONS

ANGULAR ACCEPTANCES AT HIGH P_T ($X_F > 0$)

Fig. A4

Acceptance
 $M_{NM} = 6.1$ and 9.1 GeV $\sqrt{s} = 38.7$ GeV
 $X_F > 0$ $P_T = 6.1$ GeV

Cos α dependence for different β

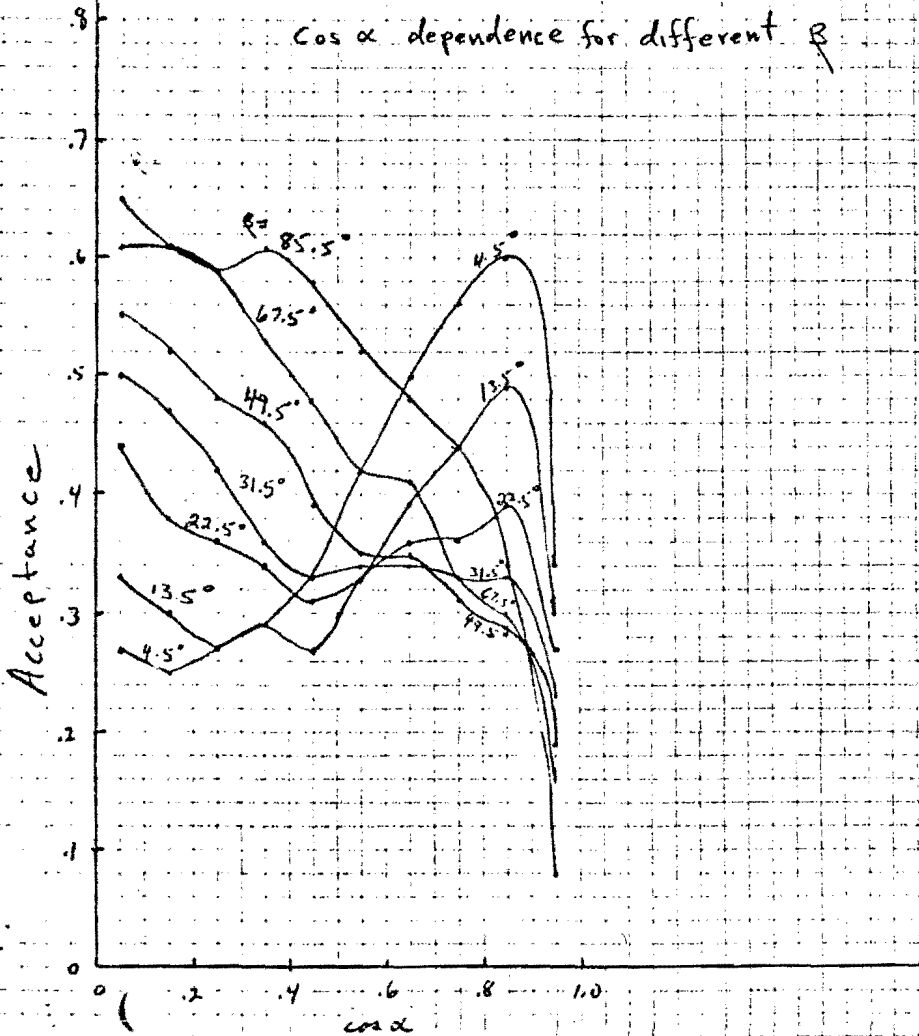
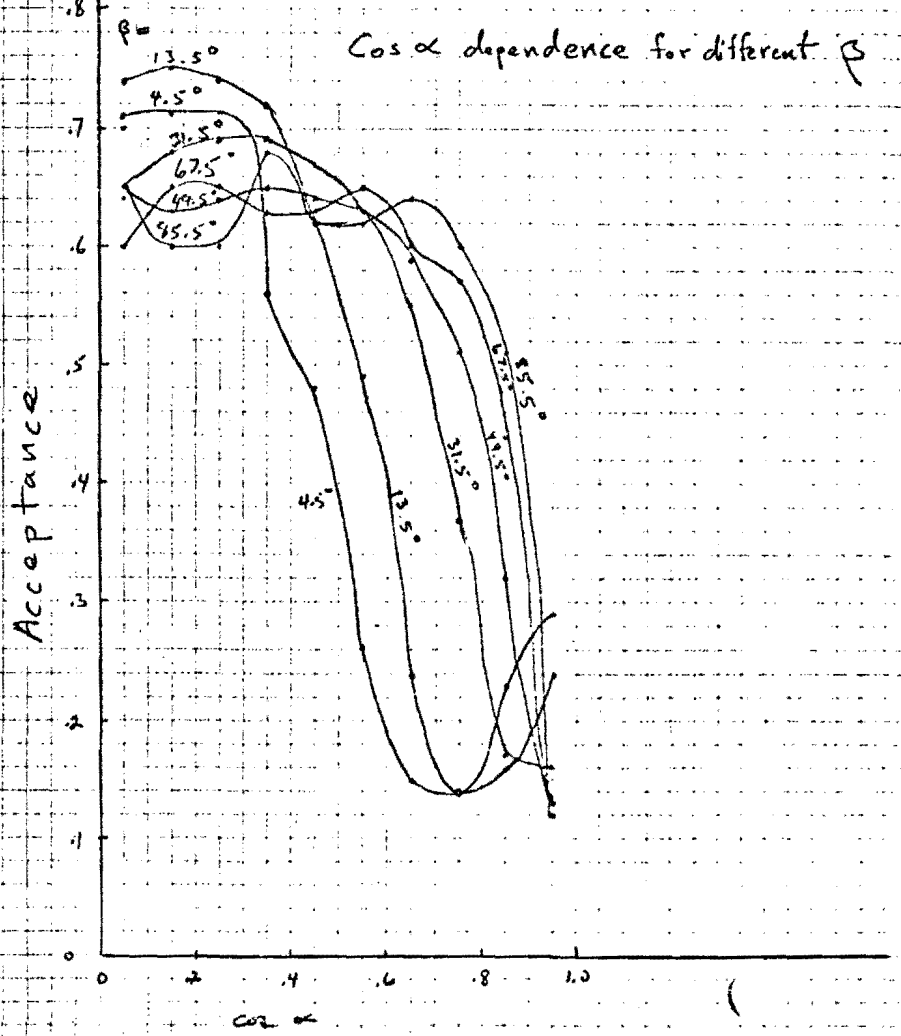


Fig. A5

Acceptance
 $M_{NM} = 6.1$ and 9.1 GeV, $\sqrt{s} = 38.7$ GeV
 $X_F > 0$, $P_T = 12.1$ GeV

Cos α dependence for different β



-15-

PROTONS
ANGULAR ACCEPTANCE LOW P_T (ASYMMETRY, DRELL YAN)

Fig. A6 $P_T^S = .75 \text{ GeV}$

Acceptance $P_T = .1 \text{ GeV}$ $\sqrt{S} = 39.7 \text{ GeV}$

$-1 < x_F < .1$
cos α dependence for different M_{MM}

-16

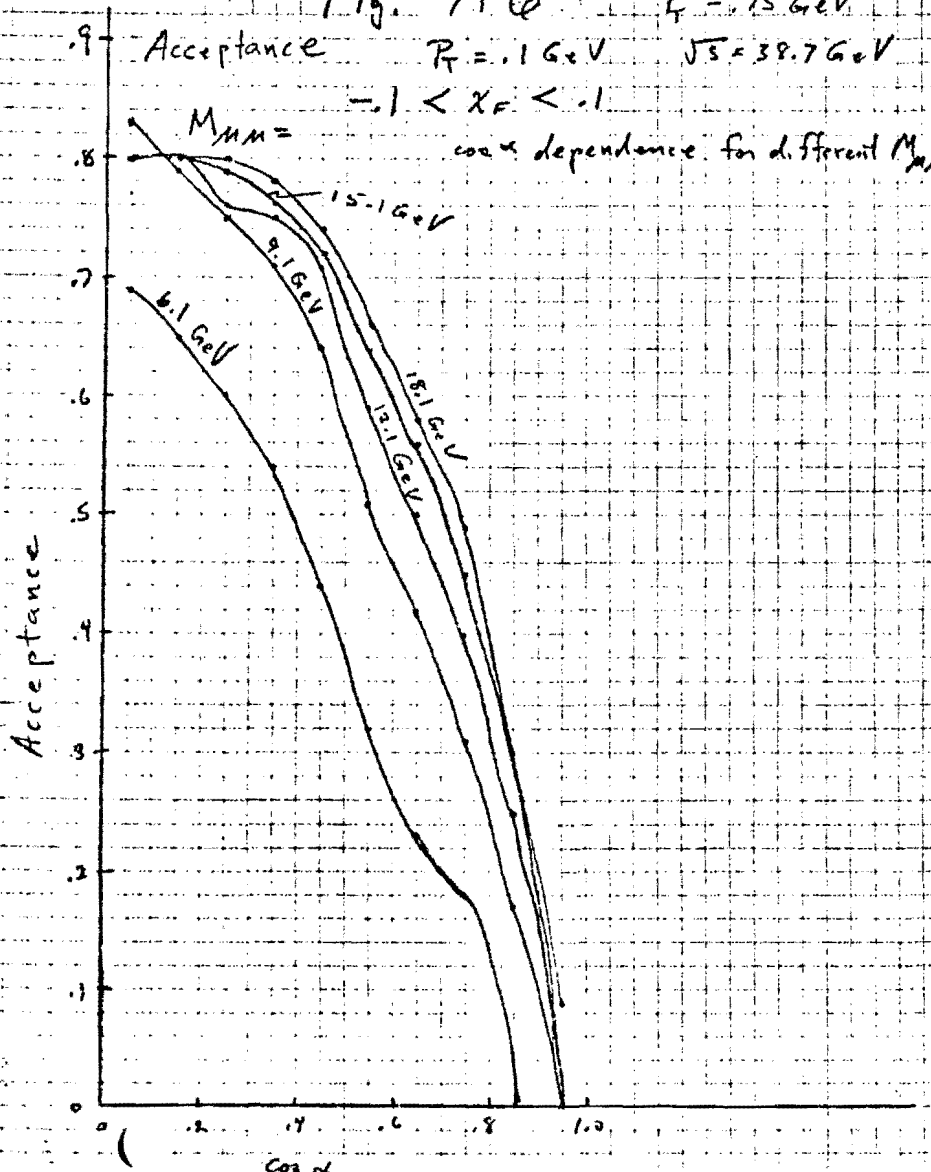
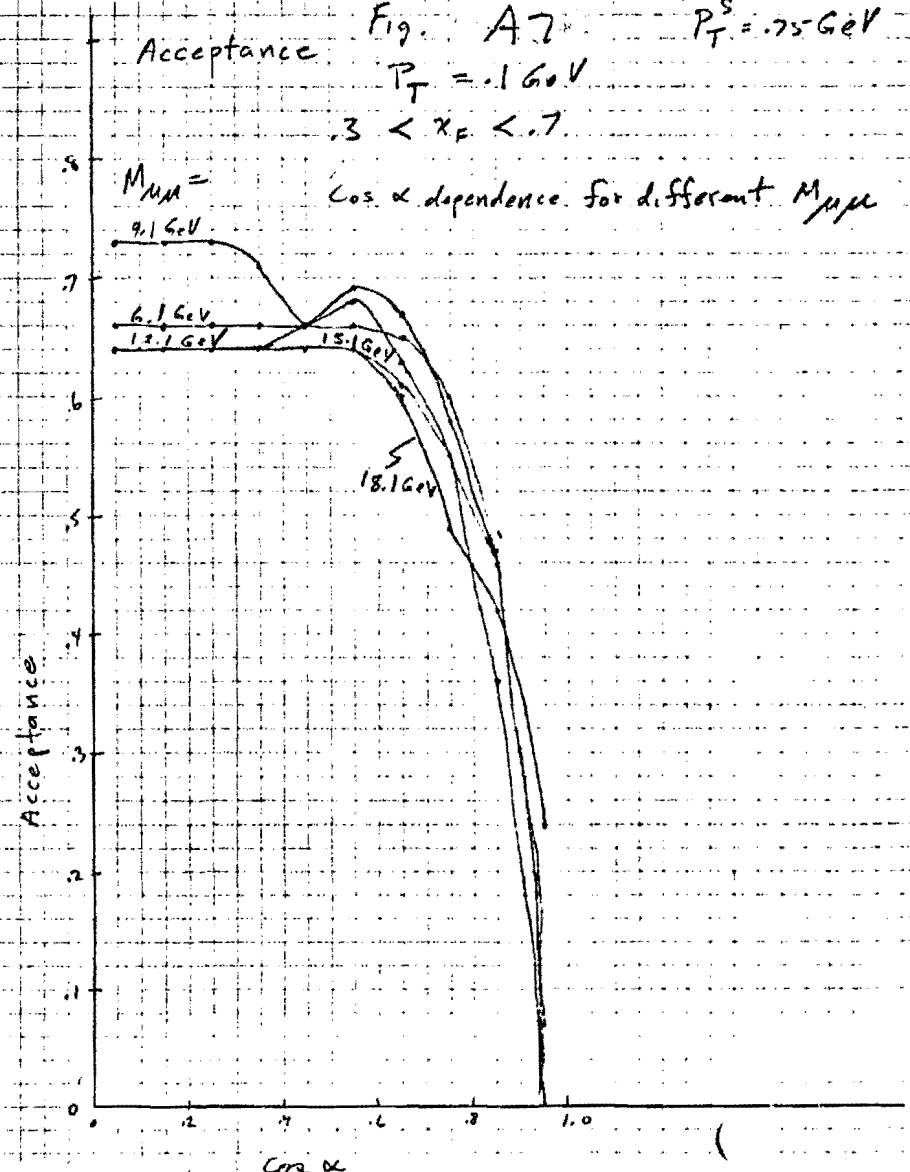


Fig. A7 $P_T^S = .75 \text{ GeV}$

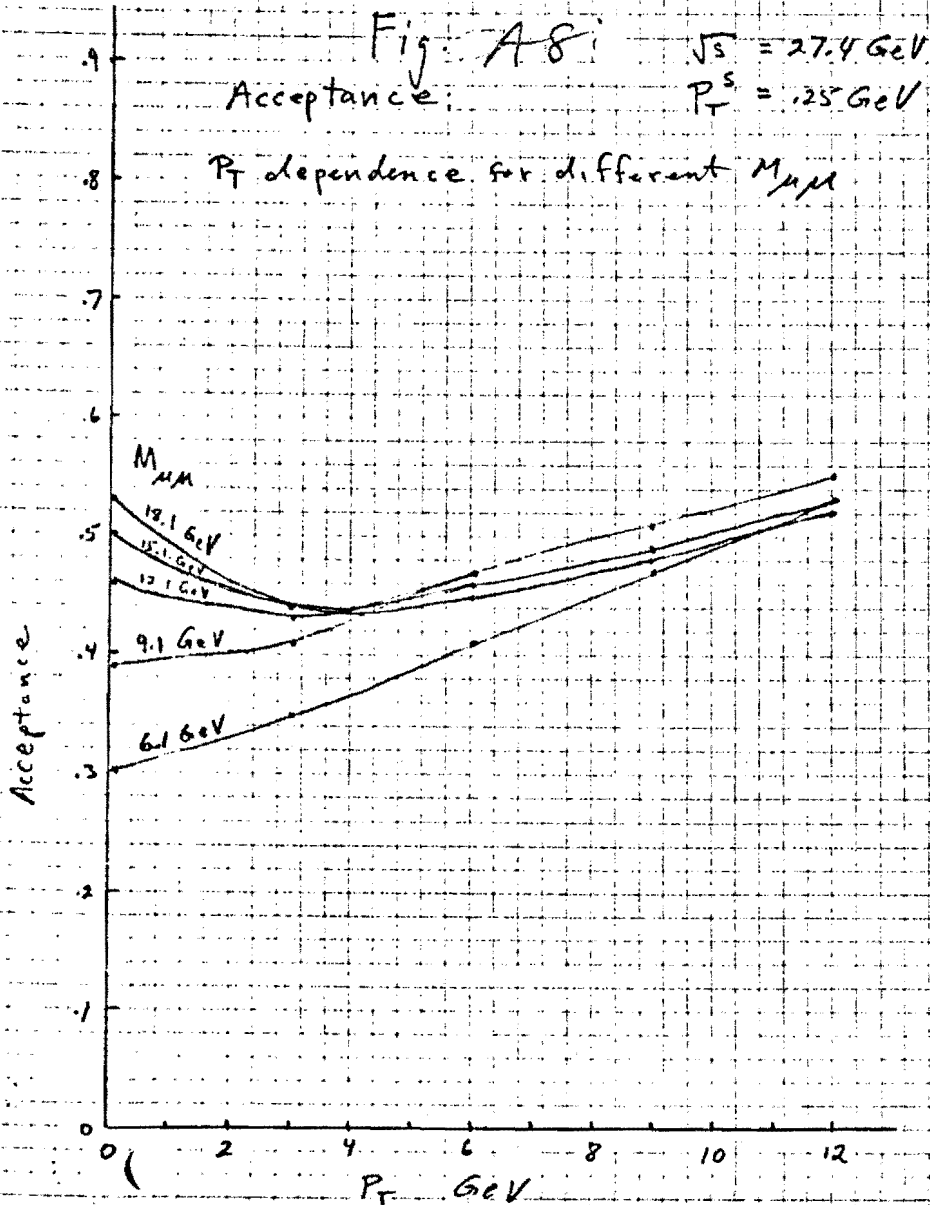
Acceptance $P_T = .1 \text{ GeV}$

$.3 < x_F < .7$
cos α dependence for different M_{MM}

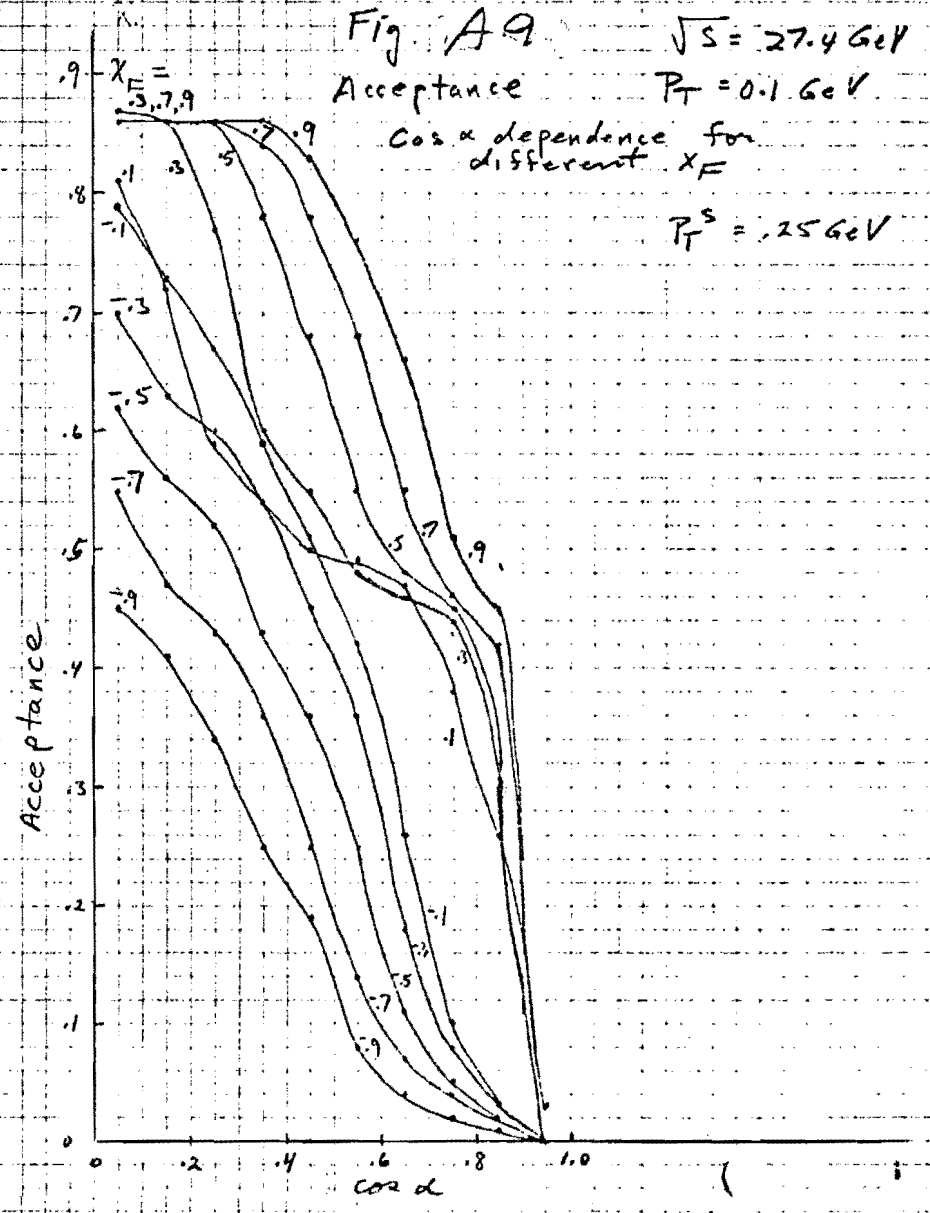


PION (400 GeV) ACCEPTANCES

P_T ACCEPTANCE



DRELL-YAN ANGULAR DISTRIBUTION AT HIGH X_F



- P 10 N BEAM ACCEPTANCES

HIGH P_T ANGULAR ACCEPTANCES $X_F > 0$

Fig. A10 $\sqrt{s} = 27.4 \text{ GeV}$
 $P_T = 6.1 \text{ GeV}$ $P_T^S = .25 \text{ GeV}$
 $X_F > 0$, $M_{\mu\mu} = 6.1 \text{ and } 9.1 \text{ GeV}$

Acceptance
 $\cos \alpha$ dependence for
 different β

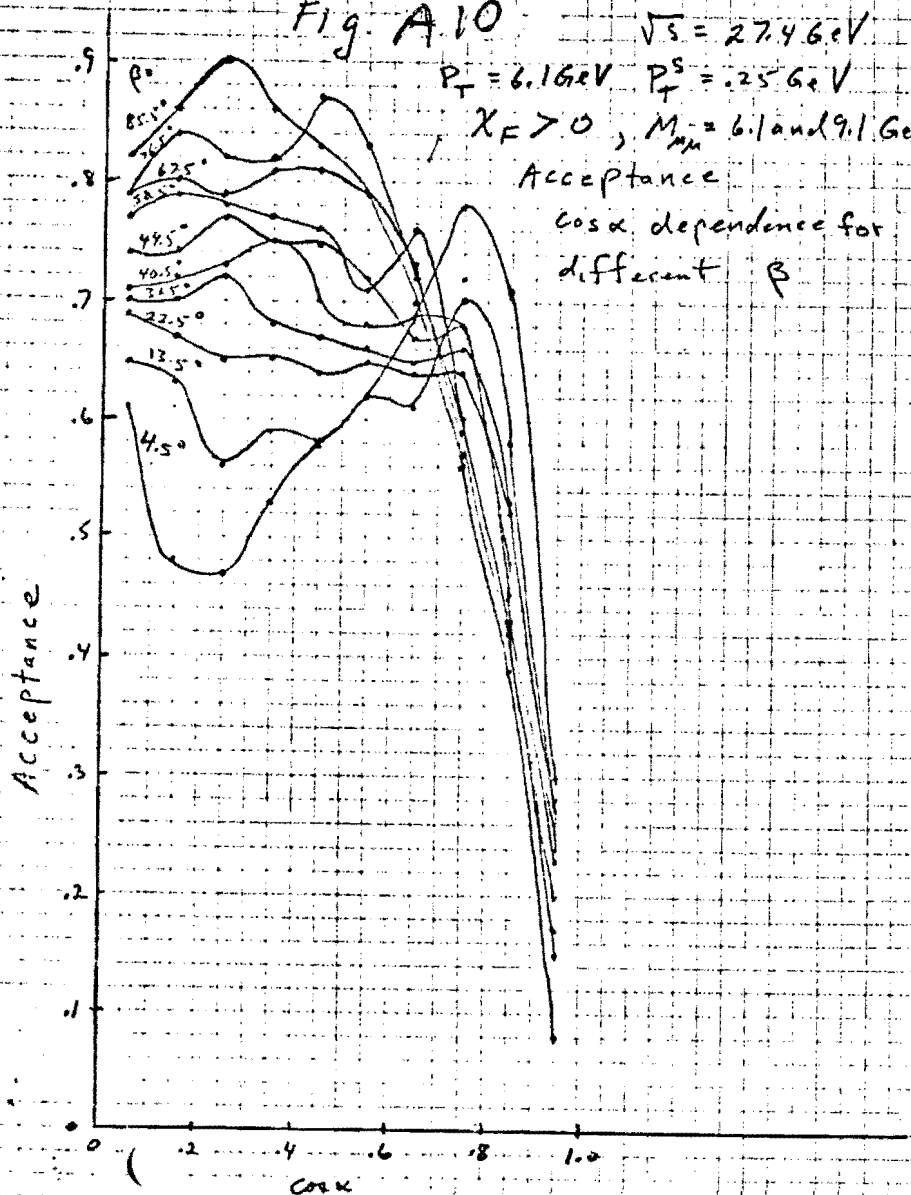
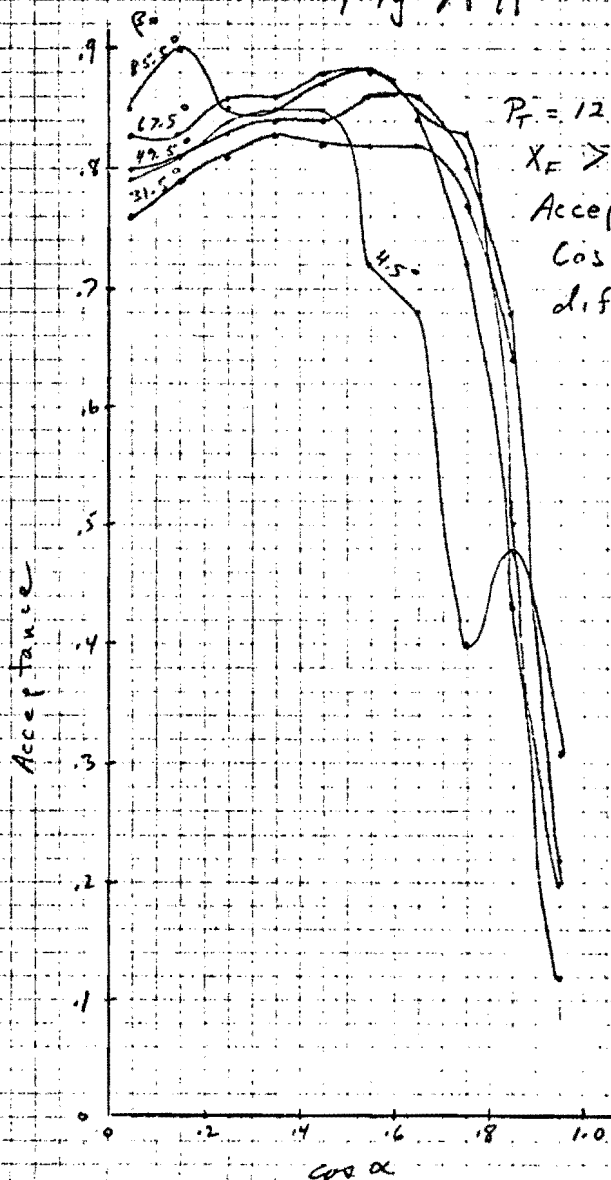


Fig. A11 $\sqrt{s} = 27.4 \text{ GeV}$
 $P_T^S = .25 \text{ GeV}$
 $P_T = 12.1 \text{ GeV}$

$X_F > 0$, $M_{\mu\mu} = 6.1 \text{ and } 9.1 \text{ GeV}$
 Acceptance
 $\cos \alpha$ dependence for
 different β



PION BEAM
HIGH P_T ANGULAR ACCEPTANCES $X_F < 0$

Fig A12

$\sqrt{s} = 27.4 \text{ GeV}$
 $P_T = 6.1 \text{ GeV}$ $P_T^S = .25 \text{ GeV}$
 $X_F < 0$ $M_{\mu\mu} = 6.1 \text{ and } 9.1 \text{ GeV}$
 Acceptance
 cos α dependence for different β

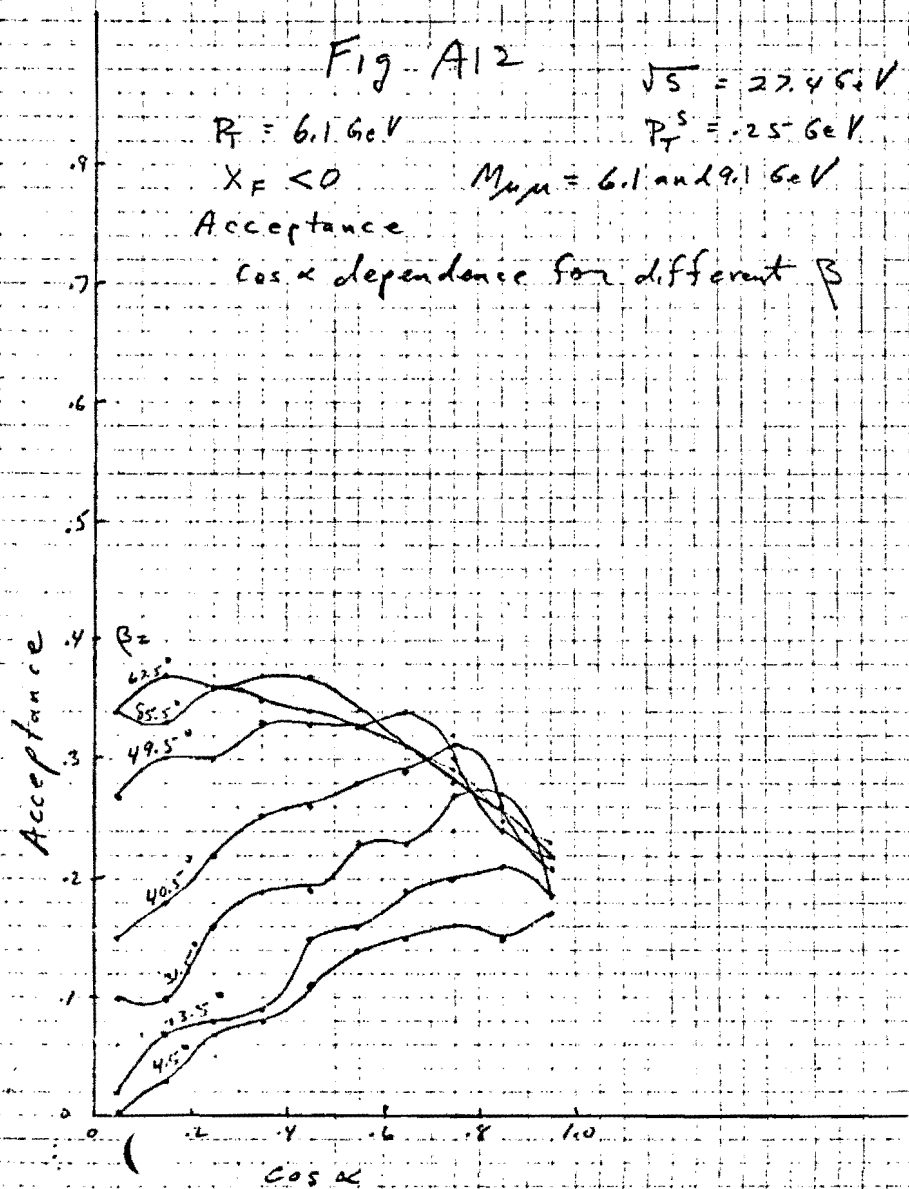
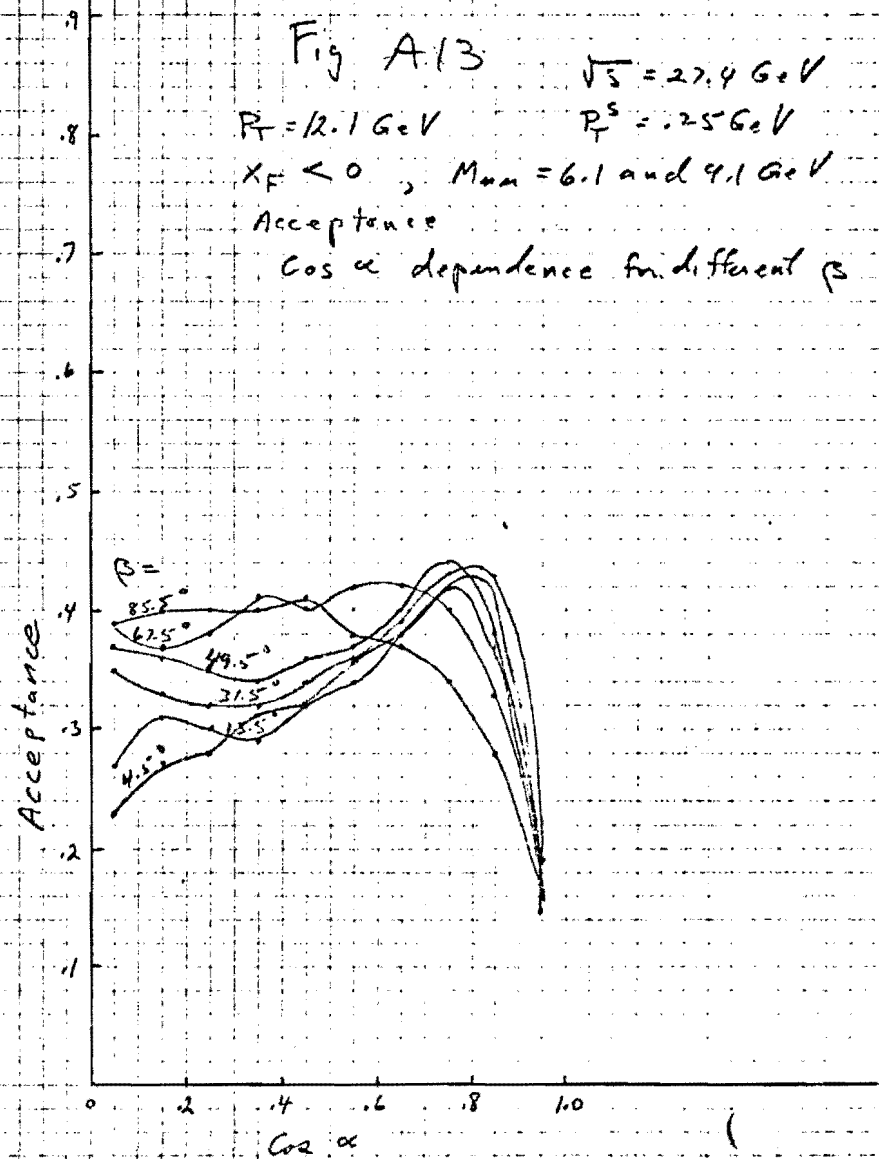
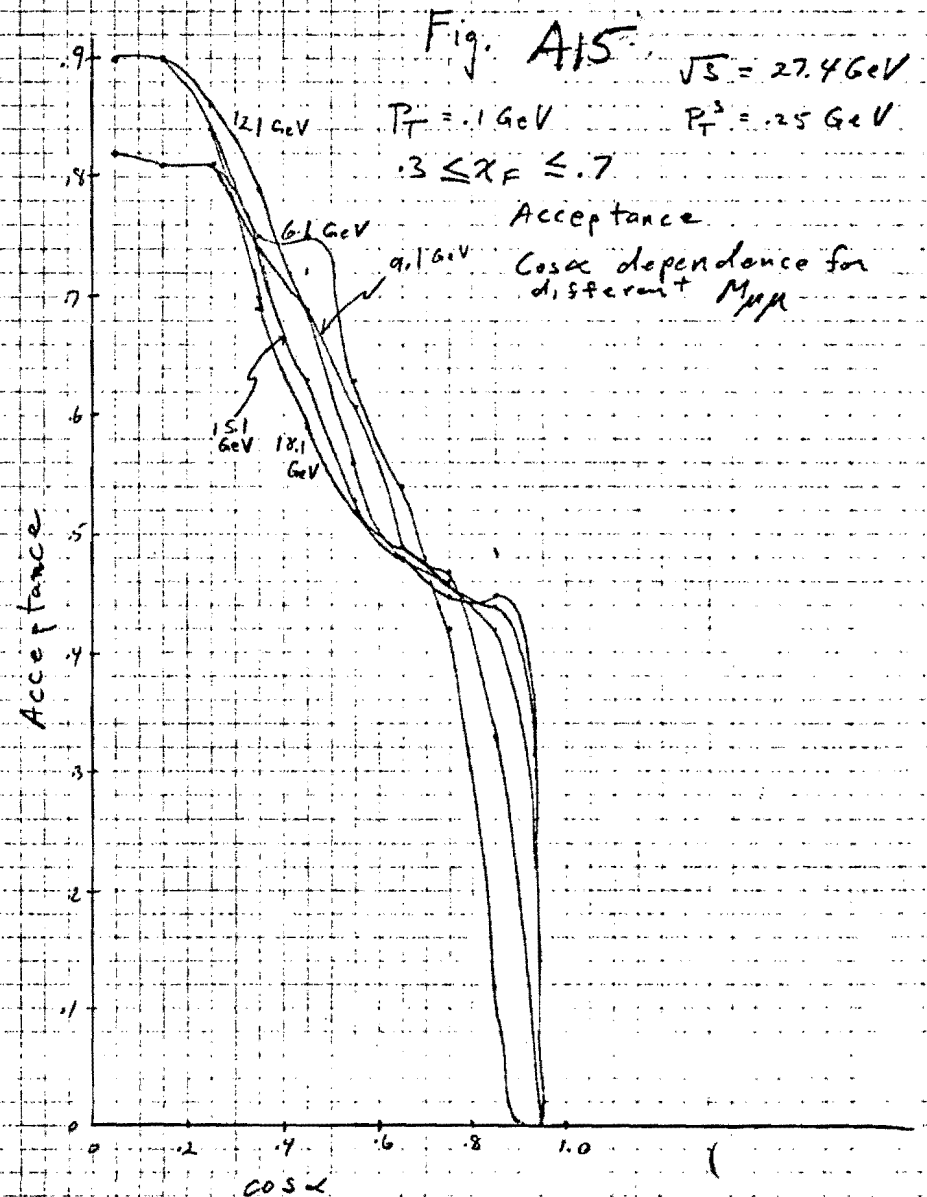
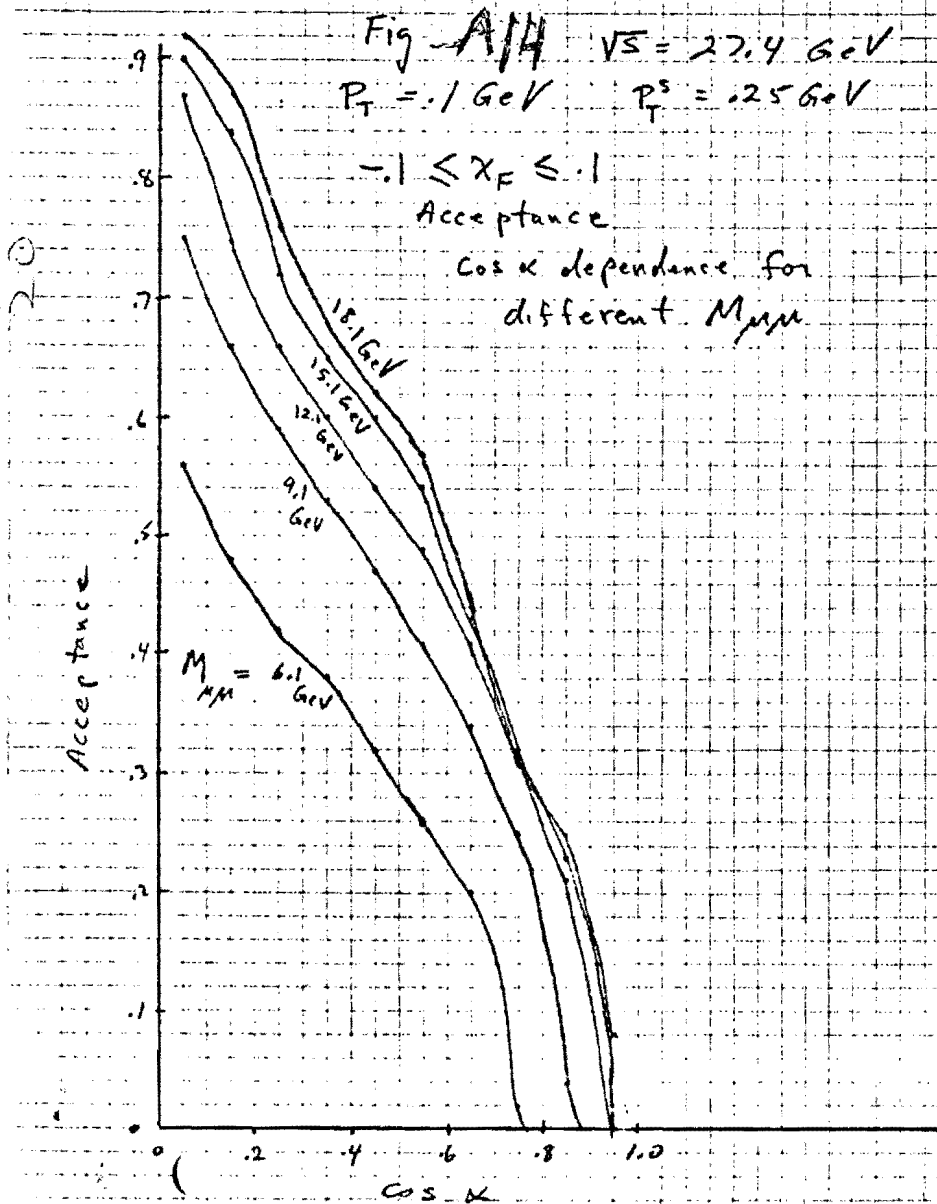


Fig A13

$\sqrt{s} = 27.4 \text{ GeV}$
 $P_T = 12.1 \text{ GeV}$ $P_T^S = .25 \text{ GeV}$
 $X_F < 0$, $M_{\mu\mu} = 6.1 \text{ and } 9.1 \text{ GeV}$
 Acceptance
 cos α dependence for different β



PION BEAM
 LOW P_T ANGULAR ACCEPTANCES
 (DRELL-YAN and ASYMMETRY)



ADDENDUM TO P-645

JUNE 12, 1980

Table of Contents:

I.	INTRODUCTION	1
II.	WHAT WILL P-645 DELIVER?	3
	II.a. General	3
	II.b. High p_T Measurements	5
	II.c. Low p_T Measurements (Drell-Yan)	13
	II.d. Weak-Electromagnetic Interference	13
	II.e. Multi- μ Production	22
	II.f. Mu-Neutrino Correlations	22
III.	LOGISTICS	24
	III.a. Apparatus and Personnel	24
	III.b. Beam	24
	Appendix I - Single μ Rates	27
	Appendix II - Neutrino Beam Dump	30

I - INTRODUCTION

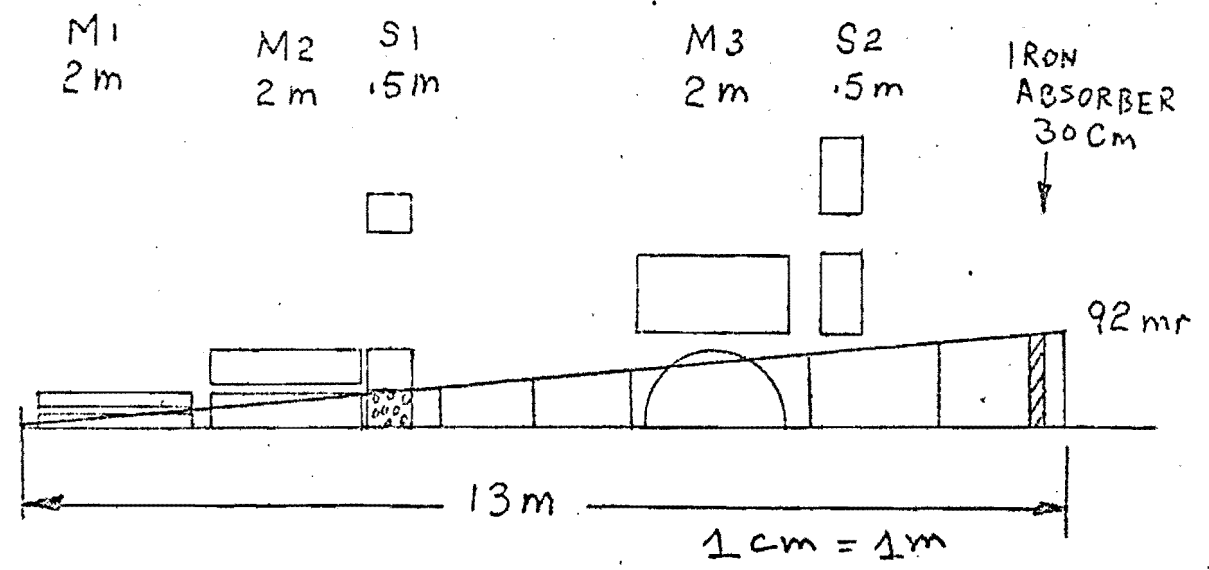
Ever since the test run of the E-439 trigger in December 1976 it has been clear to us that the E-439 type device is ideally suited for Fermilab and that it provides the most sensitive and efficient way to use the μ pair probe of hard hadronic collisions. People still find it difficult to adjust to the idea that one can have excellent acceptance (20% to 80% over most kinematic regions of interest) and yet have only two tracks pointing to the target in 60%-80% of the dimu triggered events at intensities up to 4×10^{11} protons/sec (with a 10% duty factor!). E-439 suffered from poor resolution ($> 7\%$) and poor angular acceptance (The apparatus was not big enough or elaborate enough). P-583 overcame the poor angular acceptance by adding two more stages of bending at small angles, and P-645 will overcome the poor resolution by separating the bending in the dump itself from the momentum measurement which is to be done in the detection area with the aid of a solenoid.

In response to the committee's question for our μ flux at the 15 ft bubble chamber we have reconsidered the multi-stage design that we inherited from P-583 and have concluded that it is not needed in the Tevatron era. Our experiment now consists of two iron magnets, each 2m long, which act as the beam dump, followed by a 2m solenoid with sets of drift chambers on either side and sets of hodoscopes on the far side only (Figure I). The detectors have a V (or wedge) cut, symmetric about the vertical mid-plane, the slope of the V giving the p_T cut for an individual μ to be accepted (p_T^S). The actual p_T cut we use will depend on the beam intensity (most of our physics program tolerates $p_T^S > 1.2$ GeV, but for multi- μ running p_T^S will be minimized).

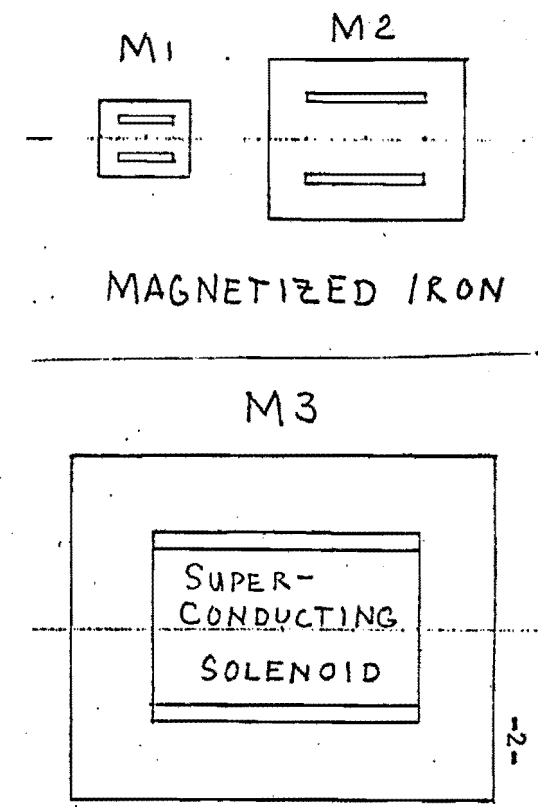
Our original approach was to set up our experiment as part of a neutrino beam dump. (The figures in Appendix II show such a beam dump when

FIGURE I

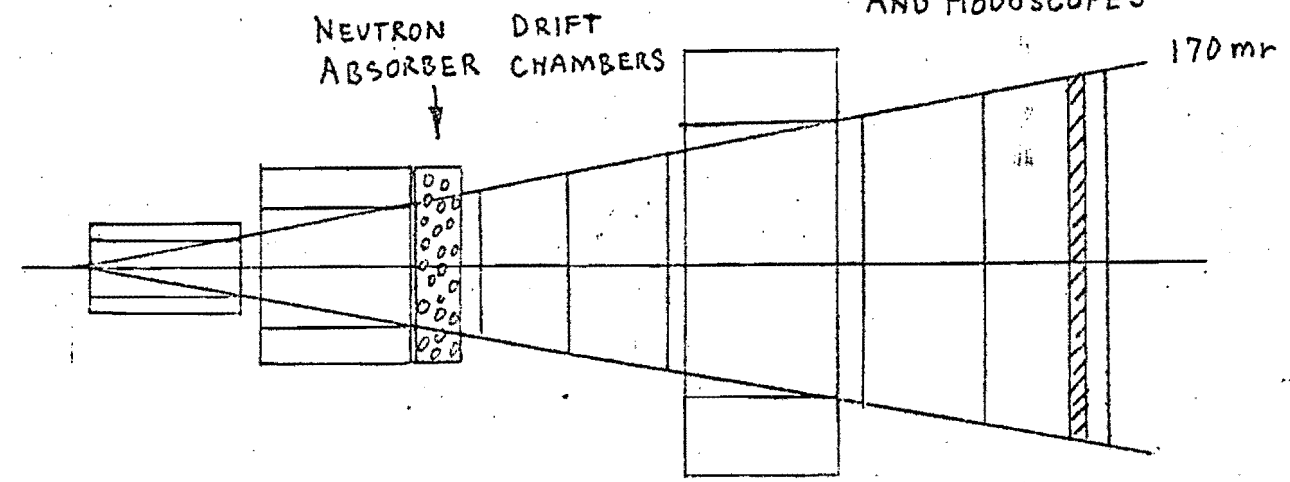
UPPER HALF VERTICAL (BEND) PLANE



MAGNET END VIEWS

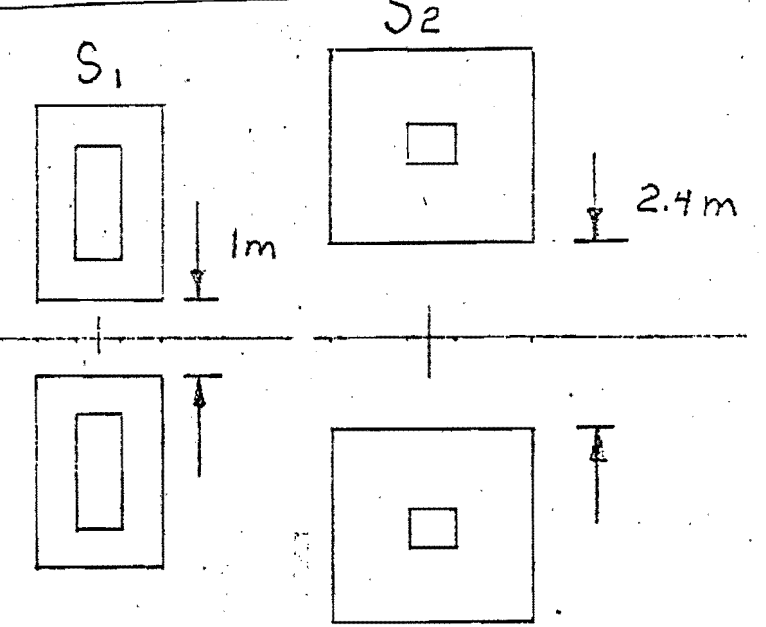


DRIFT CHAMBERS AND HODOSCOPES



MID HORIZONTAL (NON BEND) PLANE

SPOILERS



the bubble chambers are running.) However, we now consider that possibility as only one of the options or scenarios for implementing P-645. We shall discuss it, as well as implementing P-645 in the M2 line or P-West in detail below.

II. WHAT WILL P-645 DELIVER?

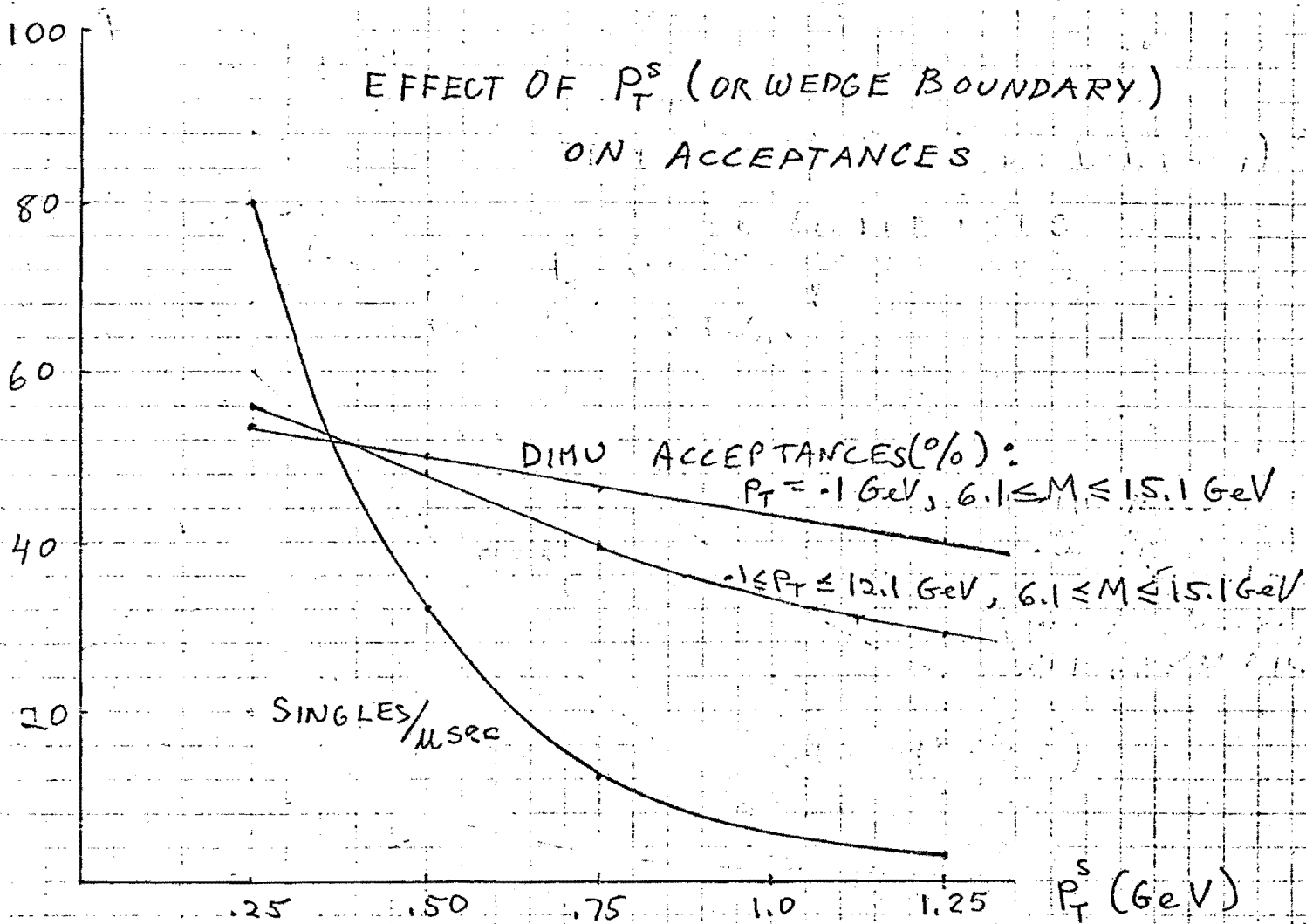
II.a. General

The momentum resolution in P-645 is about 2%; the number of radiation lengths is about 300 (not involved in the momentum resolution). The 2μ p_T resolution is .3 GeV. The mass resolution drops from 4% at 6 GeV to 3% at 9 GeV and 2% at 15 GeV and does not depend on x_F and p_T .

The singles rate in the detector depends strongly on the p_T^S cut (i.e., the slope of the wedge or V). Figure II shows the number of singles over the whole detector (62 millistrd) per μ sec, as well as overall acceptances for dimuons with masses over 6 GeV, as a function of p_T^S . The change in the singles rate as a function of p_T^S is very large and indicates the concentration of low mass events along the V boundary. The limiting factor on p_T^S in the hardware will be the average rate capacity of the individual drift chamber cell; additional constraints on triggering can be placed in the trigger logic and in the software.

Each track should register in 30 drift tubes with an off-line time resolution better than 2ns (.1 mm spatial jitter), giving 30 drift times relative to the event strobe. Eight numbers are needed for fitting two trajectories leaving 22 measured "times" for matching the track time (t_0) to the strobe time. This should peak the t_0 value by the $\sqrt{22} \sim 4$, i.e., to half a nanosecond. If we say that our off-line resolution is 1 nanosecond then the singles/ μ sec curve in Figure II divided by 10^3 gives the probability of a false track in such a one nanosecond time interval.

FIGURE II



It is important to realize that seeing the low p_T track in association with 2 higher p_T tracks cannot hurt us for the following reason. In E-439 we had a rather large p_T^S cut. Had an appreciable number of events been 3 track events in which the low p_T event got lost even though it was one member of the dimu pair we should have had an appreciable chance rate. Figure III is a typical CHANCE/TRUE = (LIKE SIGN)/(UNLIKE SIGN - LIKE SIGN) vs. intensity curve from E-439. Figure IV shows how sharply time residual like sign fraction drops with di- μ mass (i.e., with the p_T of the μ 's).

II.b. High p_T Measurements

There is no experiment anywhere that remotely approaches the capability of P-645 to measure high p_T high mass dimuons produced in hard hadronic collisions. At the P-645 presentation we gave the number of dimuons in a 1 GeV^2 mass bin per 10^{17} protons on tungsten as:

$$dN/dMdp_T = \text{Accep.} * 8 * 10^{12} e^{-.66(M+p_T)} / \text{GeV}^2 * 10^{17} \text{ protons}$$

which gives us at $M = 12 \text{ GeV}$, $p_T = 12 \text{ GeV}$, $dN/dMdp_T = \text{Accep.} * 10^{-11}$ events/ GeV^2 proton.

Figure Va shows the effect of p_T^S on the acceptance as a function of mass, p_T and the sign of x_F . Attached to it (Vb) is a two dimensional display of percentage acceptances in individual $p_T \times M$ bins for $p_T^S = .75 \text{ GeV}$. Such displays give a detailed account of the acceptance over the various kinematic ranges: all the ones we show here are for $p_T^S = .75 \text{ GeV}$ and they should all be self-explanatory. Thus, we see that the acceptance in the 12 GeV mass, 12 GeV p_T bin is 44%, i.e., for 10^{17} protons on target we will have

$$N = .44 * 10^{-11} * 10^{17} = .44 * 10^6 \text{ events.}$$

FIGURE III

MASS=8-9GEV

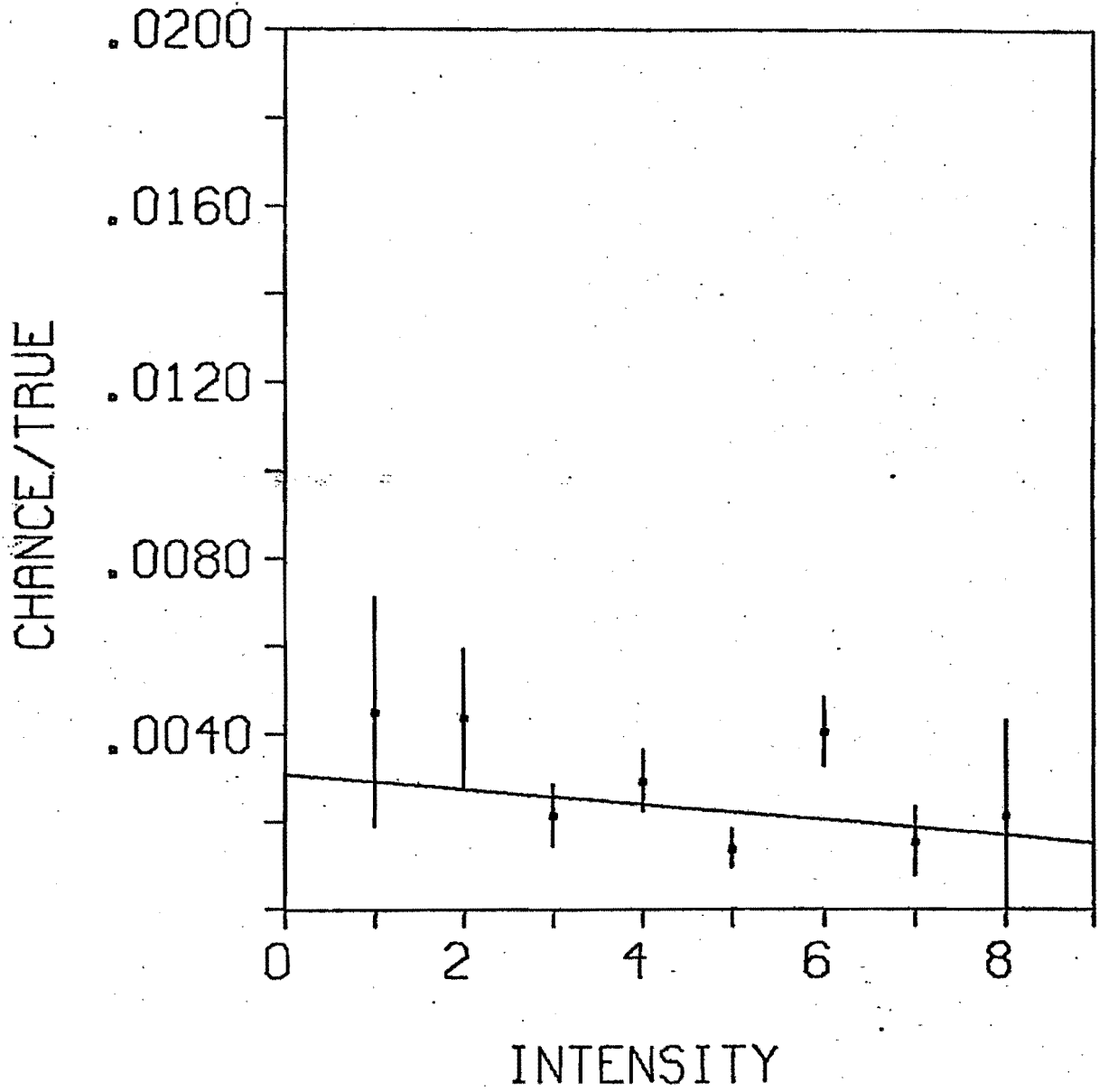


FIGURE IV

RESIDUAL VALUES (INTENSITY $\rightarrow 0$) OF
(LIKE SIGN)/(UNLIKE SIGN - LIKE SIGN)

C/T (I $\rightarrow 0$)

↑

.01

.005

.004

.003

.002

.001

0

4

5

6

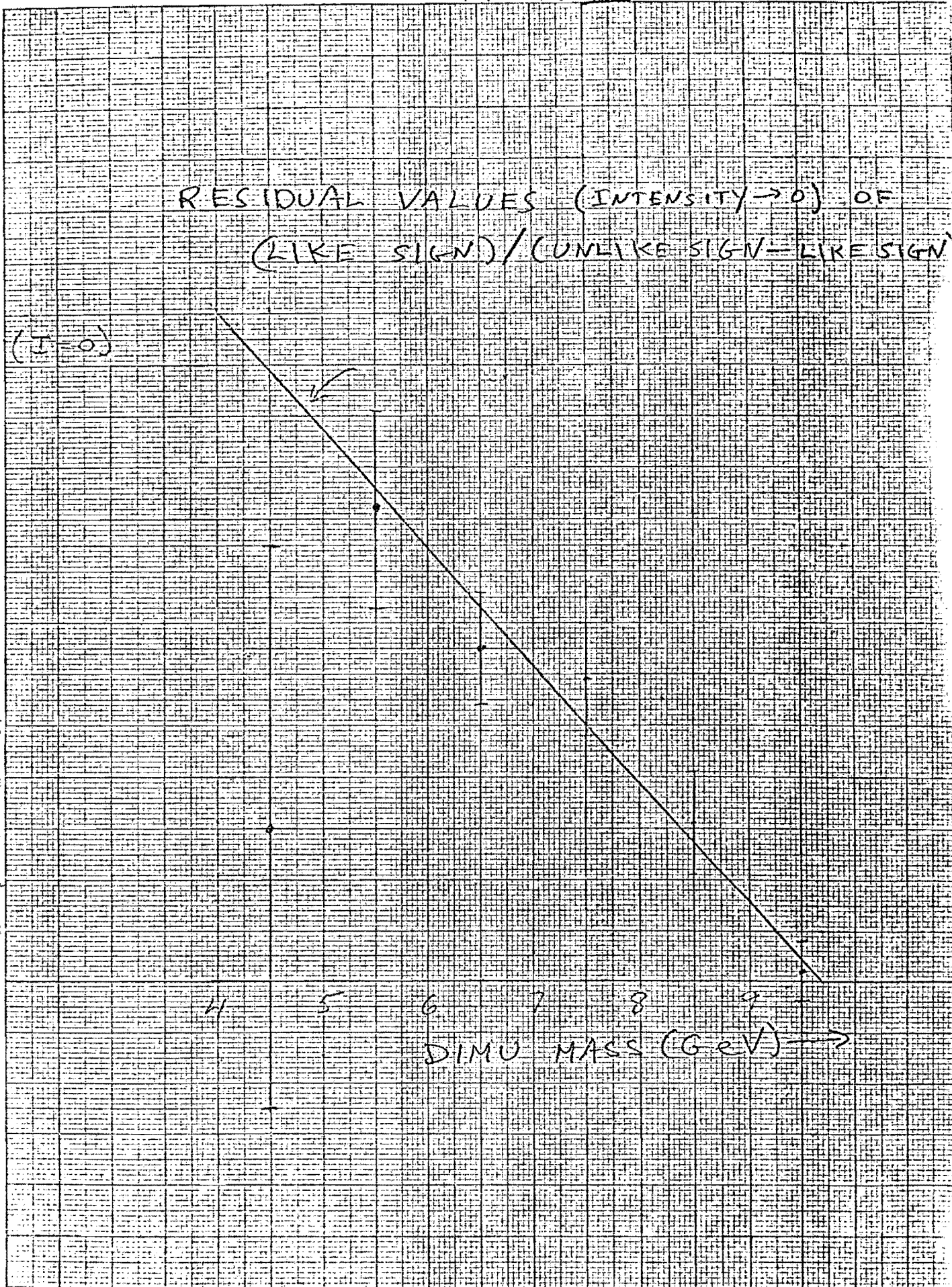
7

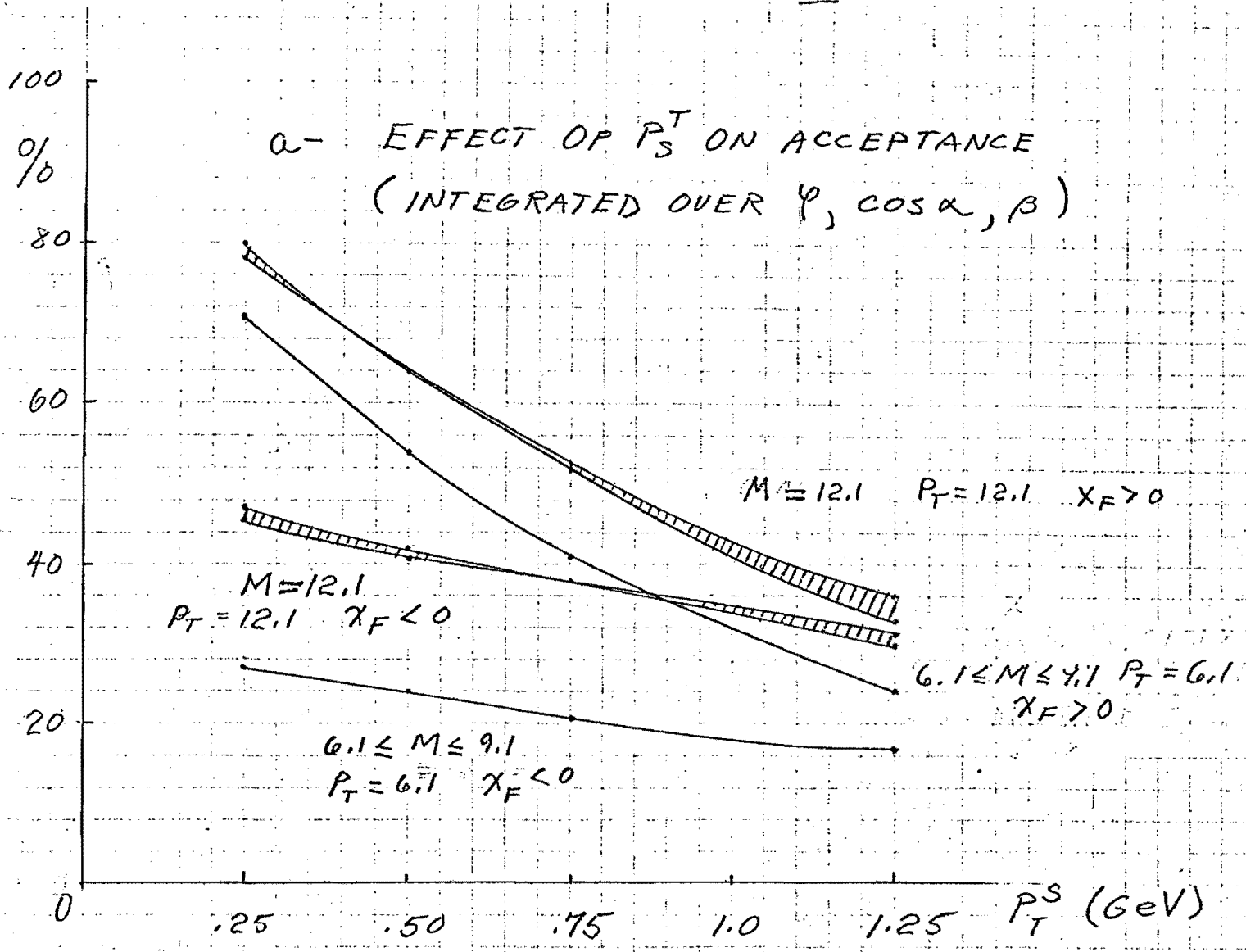
8

9

DIMU MASS (GeV) \rightarrow

10 X 10 TO THE CENTIMETER 46 1510
10 X 20 CM.
KUPPEL & EBER CO.
MADE IN U.S.A.





b - DISPLAY OF ACCEPTANCES IN P_T VS M SPACE

1 SXFULL, INDEPENDENT, GRID=5N*10XF*5PT*10PHI*10CSA*10BET*2BENDIN/OUT
BLB HGR 5 'PTVH ' PT VERSUS MASS

DATE 100680/1123

XLOC 1 X=MASS = (N_x-1)*3 + 6.1 GeV
YLOC 3
WLOC 1007 Y= P_T = (N_y-1)*3 + 0.1 GeV

BIN NOS	1	2	3	4	5
5	46.	45.	44.	41.	40.
4	37.	38.	38.	37.	36.
3	28.	34.	35.	35.	36.
2	25.	32.	36.	39.	42.
1	31.	42.	48.	52.	56.

0 194753 ENTRIES

	X-UNDER	X-NORMAL	X-OVER
Y-OVER	0.	0.	0.
Y-NORMAL	0.	.97E+03	0.
Y-UNDER	0.	0.	0.

To measure distributions in p_T , x_F , M we do not need 10^{17} protons on target. But, in addition, we have here an instrument uniquely fit to measure the dependence of the cross section on $\cos^2\alpha$ and $\cos 2\beta$ (for simplicity we defined α and β in our program in the γ^* center of mass using the direction of the p-nucleon center of mass as the new z axis ($\alpha = 0$) and the plane it makes with the beam line as the $\beta = 0$ plane). The $\cos 2\beta$ measurement is a polarization measurement; it can be measured independently as suggested by Thews (PRL 43, 987 (1979)) or in relation to $\cos \alpha$ as suggested by Devoto, et al. (PRL 43, 1062 (1979)). The precision of the measurement of an asymmetry or polarization is $1/\sqrt{2N}$, where $N = N^+ = N^-$; if $\Delta M \Delta p_T = 2$ GeV we will have at 12 GeV, 12 GeV the value $1/\sqrt{2N} = 10^{-3}$, i.e., this one range of $\Delta M \Delta p_T$ will give a precision of .001 in the asymmetry. Because of the pN asymmetry in proton-tungsten collisions it is important to do these measurements in both the forward and backward direction. In Figure VI we show 6 displays of the percent acceptance in $\cos\alpha$, β space for various masses, p_T , and x_F cuts. The data are considerably more impressive than the ones from the 3 stage detector that we showed at the May PAC presentation meeting.

Our mass resolution and p_T resolution at 12 GeV are 2.5%. Our momentum calibration is determined by the T , and the angle settings by straight tracks and survey data. Our trigger is 99.99% efficient (we require 4 out of 6 hodoscopes for a track) so we have no trigger biases aside from the p_T requirement, which at such high p_T is easy to enforce. We have very good ϕ acceptance - by varying ϕ (in the analysis) we can force the $\cos 2\beta$ distribution through different parts of the apparatus and check for possible false sources of asymmetries.

FIGURE VIa

1 SXFULL, INDEPENDENT, GRID=5H*10XF*5PT*10PHI*10CSA*10BET*2BENDIN/OUT
BLB HGR 12 'BEVCANPT' BETA VS COSA ACCEPTANCE IN GAMMA CON

DATE 100680/1123

MASTER TESTS 52 LONASS M=6.1, 9.1 55 BACK $X_F < 0$ 58 MIDPT $P_T = 6.1 \text{ GeV}$

XLOC 5
 YLOC 6 $X = \cos \alpha = N_X * 0.1 - 0.05$
 WLOC 1005 $Y = \beta = (N_Y * 0.1 - 0.05) * \pi/2$

BIN NOS	1	2	3	4	5	6	7	8	9	10
10	33.	36.	37.	35.	36.	33.	30.	27.	23.	15.
9	31.	36.	36.	36.	35.	33.	30.	27.	25.	14.
8	34.	34.	35.	34.	36.	34.	32.	27.	24.	15.
7	32.	35.	34.	33.	35.	34.	33.	30.	25.	13.
6	26.	30.	30.	29.	32.	32.	33.	29.	26.	11.
5	15.	18.	20.	20.	24.	25.	26.	28.	25.	9.
4	10.	9.	10.	17.	18.	19.	24.	22.	22.	9.
3	6.	11.	9.	9.	13.	16.	18.	19.	15.	6.
2	3.	5.	8.	9.	9.	13.	16.	9.	11.	6.
1	0.	3.	5.	6.	6.	10.	6.	5.	5.	6.

0 4295 ENTRIES

Y-OVER	0.	0.	0.
Y-NORMAL	0.	.21E+04	0.
Y-UNDER	0.	0.	0.

0 1 SXFULL, INDEPENDENT, GRID=5H*10XF*5PT*10PHI*10CSA*10BET*2BENDIN/OUT
BLB HGR 13 'BEVCANPT' BETA VS COSA ACCEPTANCE IN GAMMA CON

DATE 100680/1123

MASTER TESTS 52 LONASS M=6.1, 9.1 55 BACK $X_F < 0$ 59 HIPT $P_T = 6.1 \text{ GeV}$

XLOC 5 $X = \cos \alpha = N_X * 0.1 - 0.05$
 YLOC 6 $Y = \beta = (N_Y * 0.1 - 0.05) * \pi/2$
 WLOC 1005

BIN NOS	1	2	3	4	5	6	7	8	9	10
10	45.	41.	43.	48.	46.	45.	45.	40.	34.	11.
9	42.	41.	40.	47.	45.	45.	47.	43.	38.	12.
8	41.	38.	41.	44.	43.	45.	46.	45.	40.	13.
7	38.	39.	42.	43.	42.	43.	45.	46.	42.	11.
6	39.	40.	41.	41.	40.	43.	45.	47.	45.	11.
5	37.	38.	37.	38.	39.	43.	44.	46.	46.	11.
4	34.	36.	37.	38.	40.	42.	43.	48.	45.	7.
3	31.	35.	36.	37.	39.	43.	45.	48.	40.	5.
2	27.	32.	35.	37.	39.	43.	45.	46.	32.	5.
1	26.	30.	33.	36.	38.	40.	43.	42.	28.	5.

0 7531 ENTRIES

Y-OVER	0.	0.	0.
Y-NORMAL	0.	.38E+04	0.
Y-UNDER	0.	0.	0.

FIGURE VI b

u
 1 SXFULL, INDEPENDENT, GRID=5H*10XF*5PT*10PHI*10CSA*10BET*2BENDIN/OUT
 BL8 HGR 15 'BEVCAHPT' BETA VS COSA ACCEPTANCE IN GAMMA CON

DATE 100680/11

MASTER TESTS 52 LOHASS $M=6.1, 9.156$ FORUD $X_F > 0$ 58 MIDPT $P_T = 6.1 \text{ GeV}$

XLOC 5
 YLOC 6 $X = \cos \alpha = N_X * 0.1 - 0.05$
 ULOC 1005 $Y = B = (N_Y * 0.1 - 0.05) * \pi / 2$

BIN	1	2	3	4	5	6	7	8	9	1
HOS										0
10	65.	61.	59.	61.	58.	52.	48.	44.	34.	8.
9	63.	60.	60.	58.	55.	49.	45.	38.	31.	13.
8	61.	61.	59.	53.	48.	42.	41.	33.	30.	16.
7	60.	57.	51.	48.	44.	41.	37.	32.	30.	18.
6	55.	52.	48.	46.	39.	35.	35.	31.	29.	19.
5	53.	47.	45.	40.	37.	33.	32.	32.	31.	20.
4	50.	47.	42.	36.	33.	34.	34.	33.	33.	23.
3	44.	38.	36.	34.	31.	33.	36.	36.	39.	27.
2	33.	30.	27.	29.	27.	33.	39.	44.	49.	30.
1	27.	25.	27.	29.	33.	42.	50.	56.	60.	34.
0	8102 ENTRIES					X-UNDER		X-NORMAL		X-OVER
			Y-OVER		0.			0.		0.
			Y-NORMAL		0.		.41E+04			0.
			Y-UNDER		0.		0.			0.

Q
 1 SXFULL, INDEPENDENT, GRID=5H*10XF*5PT*10PHI*10CSA*10BET*2BENDIN/OUT
 BL8 HGR 16 'BEVCAHPT' BETA VS COSA ACCEPTANCE IN GAMMA CON

DATE 100680/11

MASTER TESTS 52 LOHASS $M=6.1, 9.156$ FORUD $X_F > 0$ 59 HIPT $P_T = 12.1 \text{ GeV}$

XLOC 5
 YLOC 6 $X = \cos \alpha = N_X * 0.1 - 0.05$
 ULOC 1005 $Y = B = (N_Y * 0.1 - 0.05) * \pi / 2$

BIN	1	2	3	4	5	6	7	8	9	1
HOS										0
10	65.	60.	60.	68.	62.	62.	64.	60.	51.	12.
9	60.	60.	66.	65.	62.	65.	62.	57.	51.	12.
8	60.	65.	65.	63.	63.	65.	60.	57.	44.	13.
7	64.	65.	63.	63.	65.	62.	59.	53.	37.	13.
6	65.	63.	64.	65.	64.	63.	59.	51.	32.	13.
5	66.	65.	66.	65.	65.	63.	58.	46.	24.	14.
4	65.	68.	69.	69.	67.	63.	55.	37.	17.	16.
3	70.	72.	74.	73.	69.	60.	45.	24.	14.	20.
2	74.	75.	74.	72.	62.	49.	24.	14.	16.	24.
1	71.	71.	71.	56.	48.	26.	15.	14.	23.	29.
0	10536 ENTRIES					X-UNDER		X-NORMAL		X-OVER
			Y-OVER		0.			0.		0.
			Y-NORMAL		0.		.53E+04			0.
			Y-UNDER		0.		0.			0.

D

FIGURE VI C

1 SXFULL, INDEPENDENT, GRID=5H+10XF+5PT+10PHI+10CSA+10BET+2BENDIN/OUT
BL8 H8R 25 'BEVCAHPT' BETA VS COSA ACCEPTANCE IN GAMMA CON

DATE 100680/1123

MASTER TESTS 53 MIDMASS M=12,155 BACK $\chi_F < 0$ 59 HIPT $P_T = 12,16 \text{ GeV}$

XLOC 5
YLOC 6 $X = \cos \alpha = N_x * 0.1 - 0.05$
 $Y = B = (N_y * 0.1 - 0.05) * \pi/2$

BIN NOS 1 2 3 4 5 6 7 8 9 0

10	50.	45.	52.	47.	47.	48.	40.	37.	32.	36.
9	45.	45.	47.	46.	45.	46.	41.	38.	32.	34.
8	41.	42.	41.	41.	43.	40.	39.	39.	34.	32.
7	41.	40.	38.	38.	38.	39.	38.	38.	34.	31.
6	41.	38.	37.	37.	37.	35.	38.	39.	34.	32.
5	39.	41.	36.	33.	33.	36.	39.	37.	35.	30.
4	41.	42.	40.	33.	33.	34.	37.	37.	36.	28.
3	22.	31.	35.	34.	30.	31.	37.	39.	33.	22.
2	17.	21.	28.	32.	31.	34.	37.	37.	28.	24.
1	14.	19.	25.	31.	31.	34.	36.	25.	21.	25.

0 3571 ENTRIES

X-UNDER	0.	X-NORMAL	0.
Y-OVER	0.	Y-NORMAL	.36E+04
Y-UNDER	0.	Y-OVER	0.

0 1 SXFULL, INDEPENDENT, GRID=5H+10XF+5PT+10PHI+10CSA+10BET+2BENDIN/OUT
BL8 H8R 28 'BEVCAHPT' BETA VS COSA ACCEPTANCE IN GAMMA CON

DATE 100680/1123

MASTER TESTS 53 MIDMASS M=12,156 FORWD $\chi_F > 0$ 59 HIPT $P_T = 12,16 \text{ GeV}$

XLOC 5
YLOC 6 $X = \cos \alpha = N_x * 0.1 - 0.05$
 $Y = B = (N_y * 0.1 - 0.05) * \pi/2$

BIN NOS 1 2 3 4 5 6 7 8 9 0

10	60.	60.	70.	60.	64.	61.	52.	47.	37.	39.
9	60.	68.	60.	60.	65.	55.	50.	42.	35.	38.
8	65.	62.	60.	65.	61.	51.	46.	38.	32.	41.
7	62.	62.	65.	60.	53.	50.	43.	36.	36.	42.
6	65.	63.	60.	55.	54.	47.	39.	31.	36.	46.
5	61.	62.	59.	57.	51.	43.	36.	35.	44.	50.
4	63.	63.	60.	54.	47.	43.	38.	41.	49.	54.
3	63.	62.	59.	52.	46.	46.	43.	46.	53.	59.
2	72.	69.	57.	48.	43.	40.	41.	46.	57.	65.
1	68.	52.	39.	31.	31.	39.	46.	56.	67.	69.

0 5184 ENTRIES

X-UNDER	0.	X-NORMAL	0.
Y-OVER	0.	Y-NORMAL	.52E+04
Y-UNDER	0.	Y-OVER	0.

0

We again remind the committee of the possibility of highly unusual effects at extremely high p_T , and that we will be able to measure the p_T dependence of the T to extremely high values (e.g., Higgs $\rightarrow \psi + \gamma$ or $T + \gamma$ giving a peak in the p_T distribution).

II.c. Low p_T Measurements (Drell-Yan)

The proposed apparatus is unparalleled in its capacity for studying x_F and angular distributions of the T and the continuum at low p_T also. Furthermore, if we are located where high intensity pion or \bar{p} beams are available it can be used for the extension of the CIP program (e.g., E-615) and the \bar{p} dimu production measurements of Cox (E-537). For these purposes there would be a distinct advantage in setting up the P-645 apparatus in P-West.

II.d. Weak-Electromagnetic Interference

It is important that the committee realize that most of the objections to P-583 are not valid for P-645.

a - The P-645 resolution is much better and the mass range, as well as the number of events per mass bin above the T , is much larger than in the original (P-583) proposal. We have a very large range (more than 10 GeV above the T) over which we expect very high yields so that the q^2 dependence of the asymmetry a (which is proportional to q^2) can be measured point to point to the third decimal place. At 18 GeV we will have

$$\frac{dN}{dM} = \text{Acceptance} \times 5.5 \times 10^{-10} \text{ events/GeV proton.}$$

Assuming that $\frac{d\sigma}{dx_F} = A(1 - |x_F|)^n$ and defining $\xi \equiv 1 - |x_F|$ then:

$$\int_{\xi_1}^{\xi_2} \frac{d\sigma}{dx_F} dx_F = A \frac{\xi_1^{n+1} - \xi_2^{n+1}}{n+1} \quad \text{and} \quad \int_{-1}^1 \frac{d\sigma}{dx_F} dx_F = \frac{2A}{n+1}$$

so at 18 GeV:

$$\frac{dN}{dM} = \text{Acceptance} * 5.5 \times 10^{-10} * \frac{\xi_1^{n+1} - \xi_2^{n+1}}{2} \text{ events/GeV proton.}$$

From E-439 $n \approx 2.7$ so for $.3 \leq x_F \leq .7$ ($\xi_1 = .7, \xi_2 = .3$)

$$\frac{dN}{dM} = \text{Acceptance} \times 7 \times 10^{-11} \text{ events/GeV proton.}$$

From the enclosed tables the acceptance at 18 GeV, "Forwd" is 81% from $\cos\alpha = -.55$ to $\cos\alpha = .55$ and drops to 46% at $\cos\alpha = \pm .85$, so taking 70% as an average, we have per 10^{16} protons (only 10^{16} protons!) 5×10^5 events/GeV which gives $\delta a = \frac{1}{\sqrt{2N}} = 10^{-3}$.

b - We also show acceptances in the central x_F region (where the asymmetry goes to zero) and in the backward hemisphere where the interference changes from being predominantly due to $u\bar{u}$ to being much more $d\bar{d}$. These different regions should allow a definitive differentiation between the physics and the systematic errors.

c - As mentioned in the recent PAC presentation, the major source of systematic error in P-583 was the fact that the vertex was used in the momentum measurement, which is not the case in P-645.

d - Should P-645 be set up where there is also a high intensity pion beam, then the asymmetry could also be measured using pion beams. Whether this will lead to a more sensitive experiment is debatable, but the theoretical interpretation of the data may be simpler. We enclose the acceptance tables for 400 GeV beam particles showing that our apparatus is suitable for angular distribution studies at that energy too.

FIGURE VII

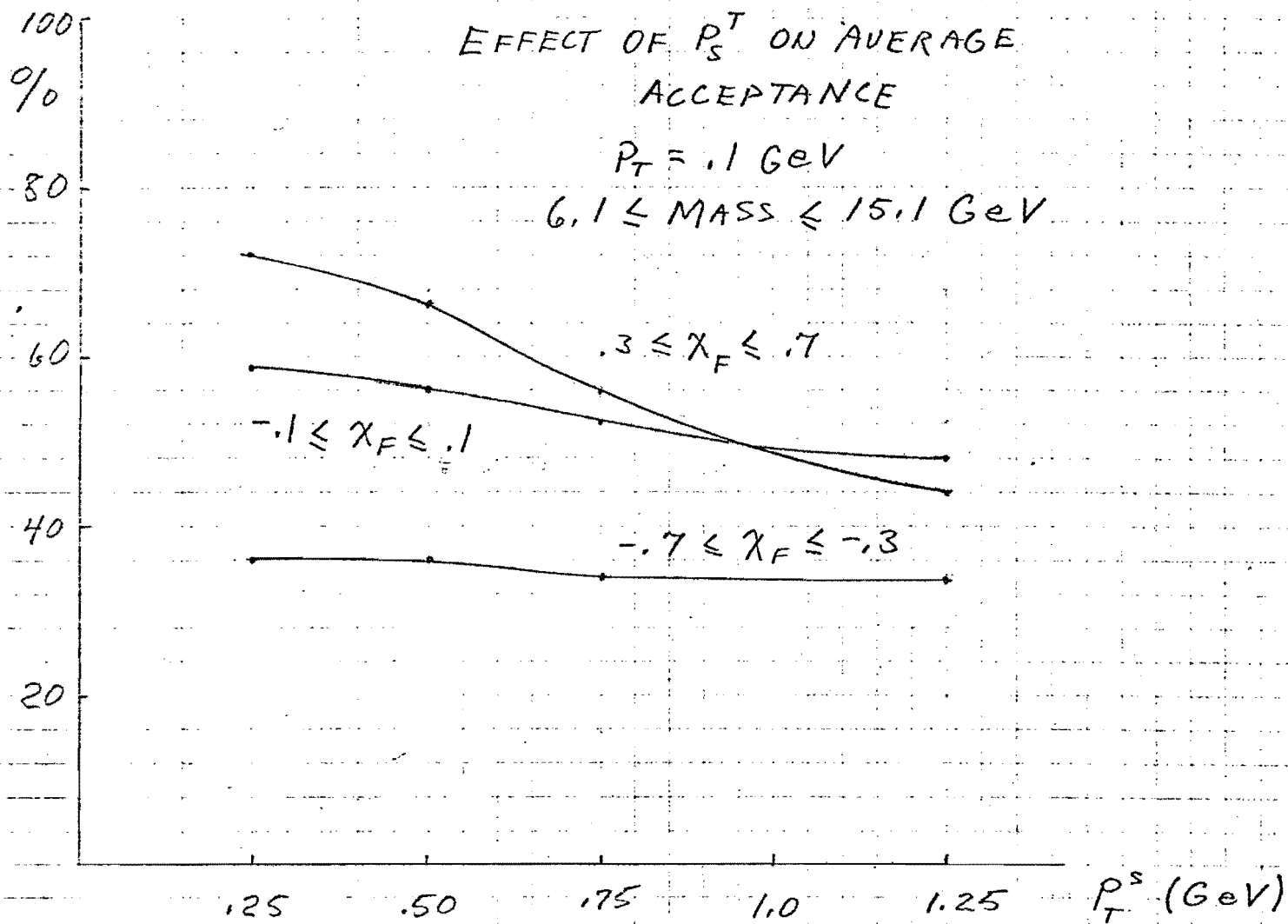


FIGURE VIII a

1 SXFULL, INDEPENDENT, GRID=5H*10XF*5PT*10PHI*10CSA*10BET*2BENDIN/OUT
BLB HGR 7 'ASYM ' ASYMMETRY REGION ACCEPTANCE

DATE 100680/112

MASTER TESTS 17 PTCUT $P_T = .1 \text{ GeV}$
XLOC 1
YLOC 5 $X = \text{MASS} = (N_X - 1) * 3 + 6.1 \text{ GeV}$
WLOC 1002 $Y = \text{COSX} = N_Y * 0.1 - 0.05$

BIN NOS	1	2	3	4	5
10	0.	0.	2.	6.	13.
9	15.	24.	25.	28.	27.
8	26.	31.	36.	38.	39.
7	30.	37.	45.	46.	51.
6	34.	43.	50.	54.	61.
5	36.	48.	56.	61.	69.
4	39.	54.	59.	68.	72.
3	41.	58.	63.	71.	74.
2	43.	61.	69.	73.	76.
1	46.	65.	70.	75.	78.

0 45761 ENTRIES

	X-UNDER	X-NORMAL	X-OVER
Y-OVER	0.	0.	0.
Y-NORMAL	0.	.23E+04	0.
Y-UNDER	0.	0.	0.

0
1 SXFULL, INDEPENDENT, GRID=5H*10XF*5PT*10PHI*10CSA*10BET*2BENDIN/OUT
BLB HSR 8 'ASYM ' ASYMMETRY BACKWARD ACCEPTANCE

DATE 100680/112

MASTER TESTS 17 PTCUT $P_T = 0.1$ 61 BACKFX $-.7 \leq X_F \leq .3$
XLOC 1
YLOC 5 $X = \text{MASS} = (N_X - 1) * 3 + 6.1 \text{ GeV}$
WLOC 1009 $Y = \text{COSX} = N_Y * 0.1 - 0.05$

BIN NOS	1	2	3	4	5
10	0.	0.	0.	0.	0.
9	0.	0.	1.	8.	10.
8	0.	1.	12.	18.	26.
7	0.	10.	24.	32.	49.
6	0.	20.	33.	49.	66.
5	2.	26.	47.	64.	73.
4	5.	36.	57.	71.	79.
3	9.	43.	65.	78.	85.
2	14.	50.	73.	83.	90.
1	19.	57.	77.	88.	94.

0 10429 ENTRIES

	X-UNDER	X-NORMAL	X-OVER
Y-OVER	0.	0.	0.
Y-NORMAL	0.	.17E+04	0.
Y-UNDER	0.	0.	0.

FIGURE VIII b

1 SXFULL, INDEPENDENT, GRID=5H*10XF*5PT*10PHI*10CSA*10BET*2BENDIN/OUT
BLB H62 9 'ASYM' ASYMMETRY CENTER ACCEPTANCE

DATE 100680/11

MASTER TESTS 17 PTCUT $P_T = .1 \text{ GeV} / 60$ CNTRFX $-.1 \leq X_F \leq .1$
XLOC 1
YLOC 5 $X = \text{MASS} = (N_X - 1) * 3 + 6.1 \text{ GeV}$
WLOC 1001 $Y = \text{COS} \alpha = N_Y * 0.1 - 0.05$

BIN NOS	1	2	3	4	5
10	0.	0.	0.	0.	9.
9	0.	17.	25.	30.	30.
8	18.	31.	40.	45.	49.
7	23.	42.	50.	56.	58.
6	32.	51.	59.	64.	66.
5	44.	64.	71.	72.	74.
4	54.	71.	75.	76.	78.
3	60.	75.	76.	79.	80.
2	65.	79.	80.	80.	80.
1	69.	83.	80.	80.	80.

0 10502 ENTRIES

	X-UNDER	X-NORMAL	X-OVER
Y-OVER	0.	0.	0.
Y-NORMAL	0.	.26E+04	0.
Y-UNDER	0.	0.	0.

1 SXFULL, INDEPENDENT, GRID=5H*10XF*5PT*10PHI*10CSA*10BET*2BENDIN/OUT
BLB H62 10 'ASYM' ASYMMETRY FORWARD ACCEPTANCE

DATE 100680/

MASTER TESTS 17 PTCUT $P_T = .1 \text{ GeV} / 62$ FRWDFX $.3 \leq X_F \leq .7$
XLOC 1
YLOC 5 $X = \text{MASS} = (N_X - 1) * 3 + 6.1 \text{ GeV}$
WLOC 1009 $Y = \text{COS} \alpha = N_Y * 0.1 - 0.05$

BIN NOS	1	2	3	4	5
10	0.	0.	0.	7.	24.
9	36.	47.	47.	46.	42.
8	55.	60.	58.	55.	49.
7	63.	65.	67.	61.	60.
6	68.	66.	69.	64.	64.
5	66.	66.	66.	64.	64.
4	66.	71.	64.	64.	64.
3	66.	73.	64.	64.	64.
2	66.	73.	64.	64.	64.
1	66.	73.	64.	64.	64.

0 16917 ENTRIES

	X-UNDER	X-NORMAL	X-OVER
Y-OVER	0.	0.	0.
Y-NORMAL	0.	.28E+04	0.
Y-UNDER	0.	0.	0.

FIGURE IX a

400 GeV $P_T^S = .25$ GeV

1 SXFULL, INDEPENDENT, GRID=5M*10XF*5PT*10PHI*10CSA*10BET*2BENDIN/OUT
BL8 HGR 5 'PTVM ' PT VERSUS MASS

DATE 120680/ 4

$$X = \text{MASS} = (N_x - 1) * 3 + 6.1 \text{ GeV}$$

$$Y = P_T = (N_y - 1) * 3 + 0.1 \text{ GeV}$$

BIN NOS	1	2	3	4	5
5	53.	55.	55.	53.	52.
4	47.	51.	51.	49.	48.
3	41.	47.	47.	46.	45.
2	35.	41.	43.	44.	44.
1	30.	39.	46.	50.	53.

0 233324 ENTRIES

	X-UNDER	X-NORMAL	X-OVER
Y-OVER	0.	0.	0.
Y-NORMAL	0.	.12E+04	0.
Y-UNDER	0.	0.	0.

1 SXFULL, INDEPENDENT, GRID=5M*10XF*5PT*10PHI*10CSA*10BET*2BENDIN/OUT
BL8 HGR 6 'CSAVXFLP ' COS(ALPHA) VS XF, PT=.1GEV

DATE 120680/ 4

MASTER TESTS 17 PTCUT $P_T = 0.1$ GeV

$$X = X_F = N_x * 0.2 - 1.1$$

$$Y = \cos \alpha = N_y * 0.1 - 0.05$$

BIN NOS	1	2	3	4	5	6	7	8	9	10
10	0.	0.	0.	0.	0.	3.	0.	0.	0.	0.
9	1.	2.	2.	3.	3.	26.	30.	33.	42.	45.
8	2.	4.	5.	8.	10.	38.	44.	45.	46.	51.
7	4.	7.	11.	18.	26.	47.	46.	48.	55.	66.
6	8.	14.	25.	36.	42.	49.	48.	55.	69.	76.
5	19.	25.	36.	45.	51.	50.	55.	68.	78.	83.
4	25.	36.	43.	54.	59.	54.	60.	78.	84.	86.
3	34.	43.	52.	60.	67.	59.	77.	86.	86.	86.
2	41.	47.	56.	63.	73.	72.	86.	86.	86.	86.
1	45.	55.	62.	70.	79.	81.	87.	86.	87.	87.

0 43725 ENTRIES

	X-UNDER	X-NORMAL	X-OVER
Y-OVER	0.	0.	0.
Y-NORMAL	0.	.44E+04	0.
Y-UNDER	0.	0.	0.

Q

FIGURE IX b

400 GeV $P_T^S = .25 \text{ GeV}$

G
1 SXFULL, INDEPENDENT, GRID=5M*10XF*5PT*10PHI*10CSA*10BET*2BENDIN/OUT
BLB HGR 15 'BEVCAHPT' BETA VS COSA ACCEPTANCE IN GAMMA COM

DATE 120680/

MASTER TESTS 52 LOMASS $M=6.1, 9.156$ FORWD $\chi_F > 0$ 58 MIDPT $P_T = 6.1 \text{ GeV}$
XLDC 5
YLOC 6 $\chi = \cos \alpha = N_x * 0.1 - 0.05$
WLOC 1005 $\gamma = \beta = (N_y * 0.1 - 0.05) * \pi/2$

BIN NOS	1	2	3	4	5	6	7	8	9	10
10	82.	86.	90.	86.	83.	79.	70.	56.	39.	8.
9	79.	84.	82.	82.	87.	83.	72.	59.	43.	15.
8	79.	80.	79.	81.	81.	79.	73.	57.	42.	17.
7	77.	79.	78.	77.	76.	71.	76.	60.	43.	20.
6	74.	74.	77.	75.	75.	72.	67.	68.	45.	23.
5	71.	72.	73.	75.	70.	68.	69.	68.	48.	24.
4	70.	70.	72.	68.	67.	66.	65.	66.	53.	27.
3	69.	67.	65.	65.	64.	65.	64.	64.	52.	24.
2	65.	63.	56.	59.	58.	62.	61.	70.	58.	28.
1	61.	48.	47.	53.	58.	64.	69.	76.	71.	30.

0 12785 ENTRIES
X-UNDER X-NORMAL X-OVER
Y-OVER 0. 0. 0.
Y-NORMAL 0. .64E+04 0.
Y-UNDER 0. 0. 0.

G
1 SXFULL, INDEPENDENT, GRID=5M*10XF*5PT*10PHI*10CSA*10BET*2BENDIN/OUT
BLB HGR 16 'BEVCAHPT' BETA VS COSA ACCEPTANCE IN GAMMA COM

DATE 120680/

MASTER TESTS 52 LOMASS $M=6.1, 9.156$ FORWD $\chi_F > 0$ 59 HIPT $P_T = 12.1 \text{ GeV}$
XLDC 5
YLOC 6 $\chi = \cos \alpha = N_x * 0.1 - 0.05$
WLOC 1005 $\gamma = \beta = (N_y * 0.1 - 0.05) * \pi/2$

BIN NOS	1	2	3	4	5	6	7	8	9	10
10	85.	90.	85.	85.	87.	88.	84.	72.	43.	12.
9	86.	89.	86.	86.	87.	87.	87.	79.	46.	17.
8	83.	83.	86.	86.	88.	89.	85.	83.	50.	20.
7	80.	83.	84.	85.	86.	87.	87.	83.	59.	21.
6	80.	81.	83.	84.	84.	86.	86.	80.	68.	20.
5	78.	81.	82.	83.	84.	86.	82.	78.	67.	19.
4	76.	79.	81.	83.	82.	82.	82.	77.	64.	22.
3	77.	78.	79.	82.	84.	83.	81.	74.	57.	24.
2	78.	81.	83.	84.	86.	82.	77.	65.	47.	25.
1	79.	81.	84.	85.	85.	72.	68.	40.	48.	31.

0 14563 ENTRIES
X-UNDER X-NORMAL X-OVER
Y-OVER 0. 0. 0.
Y-NORMAL 0. .73E+04 0.
Y-UNDER 0. 0. 0.

FIGURE IX C

400 GeV $P_T^S = .25$ GeV

1 SXFULL, INDEPENDENT, GRID=5M*10XF*5PT*10PHI*10CSA*10BET*2BENDIN/OUT
BLB HGR 12 'BEVCAMPT' BETA VS COSA ACCEPTANCE IN GAMMA CON

DATE 120680/

MASTER TESTS 52 LOMASS $M=6.1, 9.155$ BACK $\chi_F < 0$ 58 MIDPT $P_T = 6.1$ GeV

XLOC 5
YLOC 6
WLOC 1005

$$\chi = \cos \alpha = N_x * 0.1 - 0.05$$
$$y = \beta = (N_y * 0.1 - 0.05) * \pi/2$$

BIN NOS 1 2 3 4 5 6 7 8 9 10

10	34.	33.	36.	35.	34.	33.	31.	28.	26.	22.
9	35.	35.	36.	35.	34.	32.	31.	28.	25.	23.
8	34.	37.	36.	37.	37.	34.	31.	29.	25.	23.
7	33.	35.	35.	38.	35.	35.	34.	29.	25.	23.
6	27.	30.	30.	33.	33.	33.	34.	30.	24.	22.
5	15.	18.	22.	25.	26.	28.	29.	31.	26.	21.
4	10.	10.	16.	19.	19.	23.	23.	27.	27.	19.
3	6.	11.	12.	13.	16.	17.	22.	24.	25.	19.
2	2.	7.	8.	9.	15.	16.	19.	20.	21.	19.
1	0.	3.	7.	8.	11.	14.	15.	16.	15.	17.

0 4847 ENTRIES

X-UNDER X-NORMAL X-OVER
Y-OVER 0. 0. 0.
Y-NORMAL 0. .24E+04 0.
Y-UNDER 0. 0. 0.

Q 1 SXFULL, INDEPENDENT, GRID=5M*10XF*5PT*10PHI*10CSA*10BET*2BENDIN/OUT
BLB HGR 13 'BEVCAMPT' BETA VS COSA ACCEPTANCE IN GAMMA CON

DATE 120680/

MASTER TESTS 52 LOMASS $M=6.1, 9.155$ BACK $\chi_F < 0$ 59 HIPT $P_T = 6.1$ GeV

XLOC 5
YLOC 6
WLOC 1005

$$\chi = \cos \alpha = N_x * 0.1 - 0.05$$
$$y = \beta = (N_y * 0.1 - 0.05) * \pi/2$$

BIN NOS 1 2 3 4 5 6 7 8 9 10

10	39.	40.	40.	40.	41.	38.	37.	34.	28.	16.
9	38.	38.	40.	41.	42.	41.	40.	36.	32.	16.
8	39.	37.	38.	41.	40.	42.	42.	40.	33.	16.
7	37.	36.	38.	37.	38.	40.	41.	44.	39.	16.
6	37.	36.	35.	34.	36.	37.	40.	44.	38.	16.
5	38.	34.	33.	34.	35.	37.	41.	43.	41.	18.
4	35.	33.	32.	32.	34.	36.	39.	43.	43.	19.
3	31.	33.	31.	30.	33.	35.	40.	42.	44.	17.
2	27.	31.	30.	29.	32.	34.	38.	42.	42.	15.
1	23.	27.	28.	31.	32.	36.	38.	42.	37.	16.

0 5994 ENTRIES

X-UNDER X-NORMAL X-OVER
Y-OVER 0. 0. 0.
Y-NORMAL 0. .35E+04 0.
Y-UNDER 0. 0. 0.

0

FIGURE IX d

400 GeV $P_T^S = .25$ GeV

1 SXFULL, INDEPENDENT, GRID=5M*10XF*5PT*10PHI*10CSA*10BET*2BENDIN/OUT
BL8 HGR 9 'ASYM ' ASYMMETRY CENTER ACCEPTANCE

DATE 120680/

MASTER TESTS 17 PTCUT $P_T = .1$ GeV⁶⁰ CNTRFX $-1 \leq X_F \leq 1$

XLOC 1
YLOC 5
WLOC 1001

$$X = \text{MASS} = (N_X - 1) * 3 + 6.1 \text{ GeV}$$

$$Y = \text{COSK} = N_Y * 0.1 - 0.05$$

BIN NOS 1 2 3 4 5

10	0.	0.	0.	0.	8.
9	0.	4.	21.	23.	25.
8	2.	25.	32.	32.	31.
7	20.	34.	41.	43.	44.
6	26.	41.	49.	54.	57.
5	32.	47.	54.	60.	62.
4	38.	53.	60.	65.	68.
3	42.	59.	66.	72.	76.
2	48.	66.	75.	84.	87.
1	56.	75.	87.	90.	92.

0 8922 ENTRIES

X-UNDER	X-NORMAL	X-OVER
Y-OVER	0.	0.
Y-NORMAL	0.	.22E+04
Y-UNDER	0.	0.

Q 1 SXFULL, INDEPENDENT, GRID=5M*10XF*5PT*10PHI*10CSA*10BET*2BENDIN/OUT
BL8 HGR 10 'ASYM ' ASYMMETRY FORWARD ACCEPTANCE

DATE 120680/

MASTER TESTS 17 PTCUT $P_T = .1$ GeV⁶² FRWDFX $.3 \leq X_F \leq .7$

XLOC 1
YLOC 5
WLOC 1009

$$X = \text{MASS} = (N_X - 1) * 3 + 6.1 \text{ GeV}$$

$$Y = \text{COSK} = N_Y * 0.1 - 0.05$$

BIN NOS 1 2 3 4 5

10	0.	0.	0.	0.	0.
9	12.	33.	45.	44.	42.
8	42.	47.	45.	46.	46.
7	54.	49.	48.	49.	48.
6	63.	61.	56.	53.	52.
5	75.	69.	69.	63.	59.
4	75.	74.	79.	74.	69.
3	81.	81.	86.	84.	84.
2	81.	81.	90.	90.	90.
1	82.	82.	90.	90.	90.

0 17531 ENTRIES

X-UNDER	X-NORMAL	X-OVER
Y-OVER	0.	0.
Y-NORMAL	0.	.29E+04
Y-UNDER	0.	0.

II.e. Multi- μ Production

There are several open questions on how to run the multi- μ experiment in the P-645 apparatus. Should one require a minimal p_T^S so one can run at higher intensity? What will the duty factor of the Tevatron be? As pointed out in the introduction (and from Figure II), at $p_T^S = .25$ GeV the probability of an extra track in one nanosecond is .08 at 2×10^{13} protons 1 minute spill if we use the off-line time resolution of the system. On the other hand, if the Tevatron comes on for a long time with low luminosity, p_T^S could be set to 0 and multi- μ could be collected with an enormously high efficiency. In fact, P-645 is an ideal experiment for the first stage of Tevatron II operations because of its extremely high efficiency.

II.f. Mu-Neutrino Correlations

P-645 is not a proposal to measure $\mu\nu$ coincidences. However, we feel duty bound to point out to the committee that such measurements may be feasible and by using our beam dump as a prompt neutrino beam dump the option for doing these measurements in the future is left open.

Suppose we set a threshold of 40 GeV in the ν detector and assume that the ν_e ($\bar{\nu}_e$) flux in J. K. Walker's memo of 4/3/1980 is equal to the ν_μ ($\bar{\nu}_\mu$) flux, i.e., $\sim 10^6/\text{GeV} \times \text{m}^2 \times 10^{13}$ protons at Lab. C. Using a ΔE_ν of 60 GeV (40-100 GeV, $\bar{E}_\nu = 70$ GeV) and 16 m^2 for the LABC detector, we have $10^9 \nu/10^{13} \text{ p}$. The probability of detecting a 70 GeV neutrino going through $3 \times 10^3 \text{ g/cm}^2$ is $70 \times 1.8 \times 10^{-11} \approx 10^{-9}$ so one would have one prompt ν per 10^{13} protons.

From Figure II (and the discussion in Section IIa, the probability of a μ track in 1 nanosecond per $2 \times 10^{13}/\text{minute}$ is .082 (for $p_T^S = .75$), i.e., for $10^{13}/\text{sec}$ it will be only .36. If we assume that 10% of the μ 's

associated with prompt $\nu_{\mu} = 70 \pm 30$ GeV will have a $p_T > .75$ GeV we can have a $\mu\nu$ event per 10^{14} protons with a 2 to 1 probability of it not being a chance coincidence. If the off-line resolution is .5 nanosecond the signal becomes cleaner. One can see the possibility of 10^3 $\mu\nu$ coincidences for 10^{17} protons on target.

The problems are formidable. The ν detectors will have to take beam in at least a full second spill, something which only E-613 is doing at this time. The drift cells along the p_T^S boundary will have recovery problems which will require great technical skill to handle. Also, the signals from the μ detection will have to be delayed ~ 1 μ sec before they are latched. Nevertheless, we believe that all these difficulties can be overcome if the effort is considered worthwhile. Again, we emphasize: we do not propose to do it at this time -- we only wish the committee to be aware of the potential for this physics.

III. LOGISTICS

III.a. Apparatus and Personnel

In terms of physics, beam occupancy and experimental lifetime P-645 is a mammoth proposal. In terms of costs and demand on equipment it is moderate. The solenoid (exclusive of return yoke) should cost between \$500 K and 750 K and since it is only 2T it is the easiest kind of superconducting magnet to build. The return yoke, as well as the other magnets and spoilers are supposed to be very cheap because of the Argonne steel - they should not cost more than 300 K. The hodoscopes are just more of what we had in E-439 (175 → 750 elements) and should cost less than \$250 K. The drift cells, of which we have 7,500, are the type used in Lab C and were estimated last year at \$15/cell so 150 K is a conservative estimate for them. The electronics, cabling, on-line computer, etc., is standard also. We apologize for not having a complete worksheet of costs and tasks, with associated dates all worked out. We feel that first the key decisions have to be made on whether the Laboratory should pursue this program and in what beam line and what time frame, before we start working out the additional details.

The same holds for the group size and its competency to do the experiment. George Glass, a highly experienced high energy physicist will join our group and spend next year at Fermilab working on this proposal. If the Laboratory indicates its support for this program many other groups will join us and by the time the Laboratory is ready to develop an agreement the enlarged collaboration will be ready too.

III.b. Beam

We consider 3 alternative scenarios; the order in which they are presented does not reflect our preference.

1 - P-West is upgraded to receive primary extracted beam and the \bar{p} and pi experimenters agree to use the P-645 apparatus for their measurements. In that scenario the P-645 system is left in situ for years, beginning with Saver (500 GeV proton physics and lower momentum secondary beams), through the first stage of Tevatron II, when the extracted beam will be used to maximum efficiency by the high acceptance of P-645, to the full range of the P-645 program as Tevatron II turns out more protons. Since P-645 is compatible with E-613, a possible solution to continuing E-613 if a beam dump is not built in the neutrino line, would be to place E-613 downstream of P-645 in p-West.

2 - P-645 is set up in the M2 line in front of E-613 and the polarized beam is built elsewhere. Unfortunately, M2 does not have the capacity for high intensity secondary beams.

3 - P-645 is placed in the prompt neutrino line as part of the neutrino beam dump (Appendix II). The difficulty here lies in the fact that the slow spill running contemplated by the neutrino experimenters is still at a rate of 10^{14} /sec. Whether they can be reoriented towards longer spills [in the hope of running $\mu\nu$ coincidences at a future date] is a doubtful proposition. On the other hand, there is the option of running P-645 when they are studying decay neutrinos. In that case the beam line would be developed well before the full capacity of the Tevatron II is achieved. P-645 could start running with the 500 GeV Saver beam, trickles of Tevatron II beam (useless for neutrino physicists) and slow spill when Tevatron II is in full operation and conventional neutrino running is on.

Thus, finally, we come to the question posed to us by the PAC: What is the muon flux from our dump design at the 15' bubble chamber? We have given our design (Appendix II) to the MIT (30") group to test out;

unfortunately their computer was down and as of this moment we do not have the answer. This design should be considered as preliminary in any case; we will be working with the MIT group in the next few weeks and hope to have a proper answer for the committee.

We hope that the committee will contact us for any details and additional information. Our office phones are:

(617) 437-2933 (Glaubman),

437-2936 (Garellick),

437-2902 (Physics Office) and

(617) 861-9443, or 8615 (Glaubman) and

(617) 469-0980, 325-1644 (Garellick) .

We will be glad to provide information at any time of the day, any day.

Appendix I

Single μ Rates in P-645 Detector

Anderson et al. give the single μ rate in pBe at 150 GeV from dimu production (PRL 37, 803 (1976)). For the purposes of crudely estimating our rates this should yield reasonable values. We further assume that the rates scale as $\ln s = 1.7$, that the Be μ production is $A^{2/3} \approx 4$ times the nucleon μ production, that the ratio of W μ production to total cross section is $A^{1/3} = 5.6$ times the ratio of nucleon μ production to total cross section of $50 \text{ mb} = 5 \times 10^4 \mu\text{b}$. (At low mass the dimu production seems to have the same A dependence as hadronic production. We leave the factor of 5.6 in as a margin of safety to compensate for dimu production by secondaries.) If F is the number of microbarns of cross section given by Anderson et al. and Y is the μ yield per proton on the beam dump then:

$$Y = \frac{1.7 \times 5.6 \times F}{4 \times 5 \times 10^4} .$$

The number produced per second from a one minute spill of 2×10^{13} protons

$$N = \frac{2 \times 10^{13}}{60} \quad Y = 1.6 \times 10^7 F .$$

We obtain F for individual mass, x_F and p_T bins from the following table based on Anderson et al. (They fit to a $d\sigma/dp_T^2 \propto e^{-bp_T}$ and $\frac{d\sigma}{dx_F} = A (1-x_F)^c$ distribution. We extend this assumed distribution to negative x_F by putting $\frac{d\sigma}{dx_F} = (1 - |x_F|)^c$ and combine the resonance yields with those of the continuum at the proper masses.)

Table 1

(A in μb , M in GeV, b in GeV^{-1})

I	\bar{M}	ΔM	A	b	c
1	.3	0 - .45	62	4.6	8.3
2	.5	.46 - .65	20	4.6	6.5
3	.79	$\rho + w + .65 - .93$	16.3	3.8	4.3
4	1.03	$\varphi + .93 - 1.13$	3.6	3.9	5.6
5	1.56	1.13 - 2	.64	4.1	5.1

In terms of our bins (normalizing the p_T distribution and integrating over x_F and p_T) the cross section for a bin is:

$$F(\bar{M}, \Delta M, \bar{x}_F, \Delta x_F, \bar{p}_T, \Delta p_T) = F(I, \xi_1, \xi_2, n) =$$

$$= A(I) \frac{1 + 2n}{e^{2n}} \left(1 - \left(1 + \frac{2}{1 + 2n} \right) / e^2 \right) \frac{\xi_1^{c+1} - \xi_2^{c+1}}{c + 1}$$

where $\bar{M} = \bar{M}(I)$, $\Delta M = \Delta M(I)$, $c = c(I)$, $b = b(I)$ and:

$$\xi_1 \equiv 1 - |\bar{x}_F| + \frac{1}{2}\Delta x_F, \quad \xi_2 = \xi_1 - \Delta x_F,$$

$$\bar{x}_F = -1 + (m + .5)\Delta x_F, \quad m = 0, 1, \dots, (2/\Delta x_F - 1)$$

and:

$$\Delta p_T = 2/b(I), \quad \bar{p}_T = (2n+1)/b(I) = (n+\frac{1}{2})\Delta p_T, \quad n = 0, 1, 2, \dots$$

We used five p_T bins and 10 x_F bins ($\Delta x_F = .2$), thus giving us 250 bins in which to calculate μ production according to the formula for F.

To obtain the rate of single μ 's in our apparatus, our program generated 2000 μ pairs in each bin, 10 for each angle variable ($\varphi, \cos\alpha, \beta$)

and one each for bend in/bend out. If on tracking a μ hit the back detector the event was recorded and a number, $W = 1000 * F$ was attached to the event. In addition to using these numbers for weighing x, y displays they were summed (S) to give the total number of μ 's hitting the detector.

$$8 \times S = 8 \times 2000 \times 1000 \sum_{M, P_T, x_F} F \times \text{Acceptance}$$
$$= 1.6 \times 10^7 \sum F \times \text{Acceptance}.$$

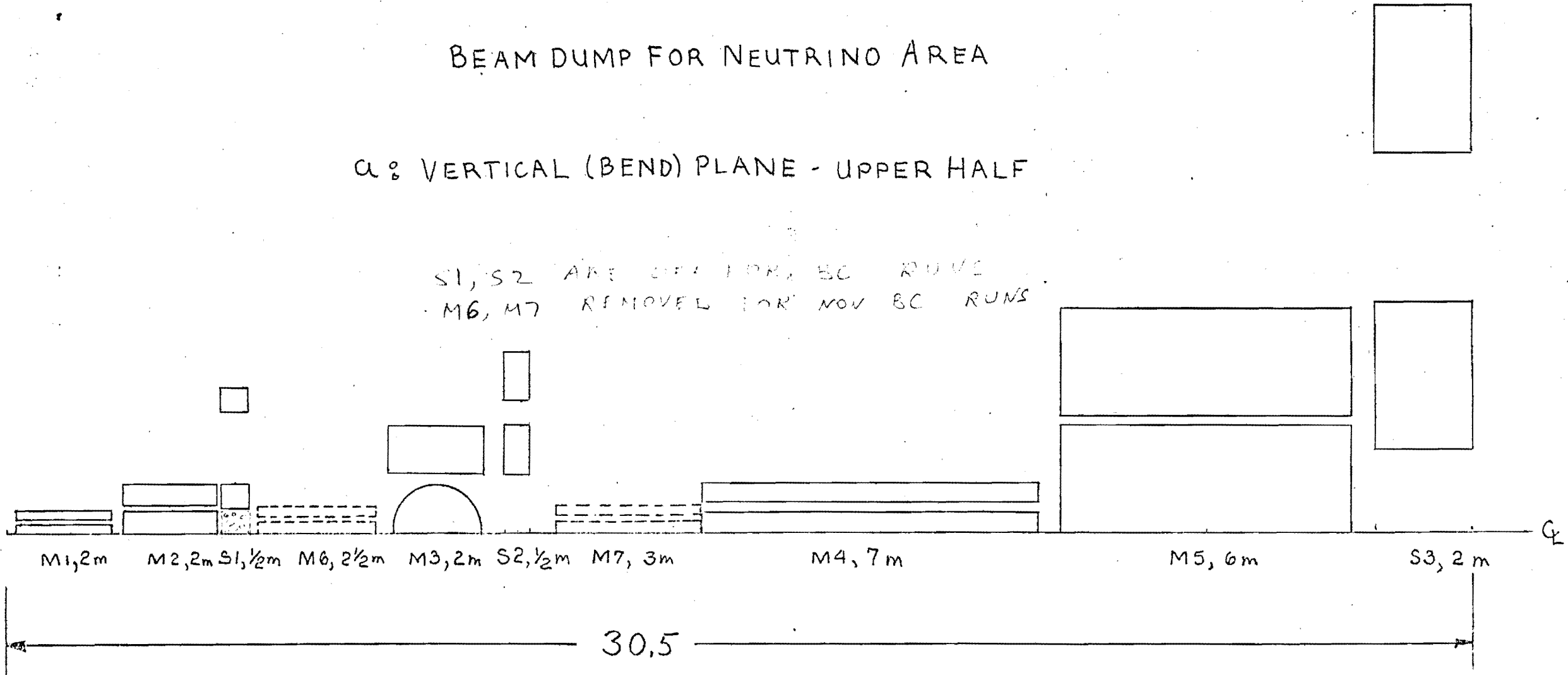
Since $1.6 \times 10^7 \sum F = \mu$ yield/second from 2×10^{13} per minute protons of 800 GeV on tungsten, $8S = \mu$ rate in our detector. These are the single rates we use for various p_T^S in Figure II.

APPENDIX II

BEAM DUMP FOR NEUTRINO AREA

α: VERTICAL (BEND) PLANE - UPPER HALF

S1, S2 ARE OFF FOR BC RUNS
 M6, M7 REMOVED FOR NOV BC RUNS



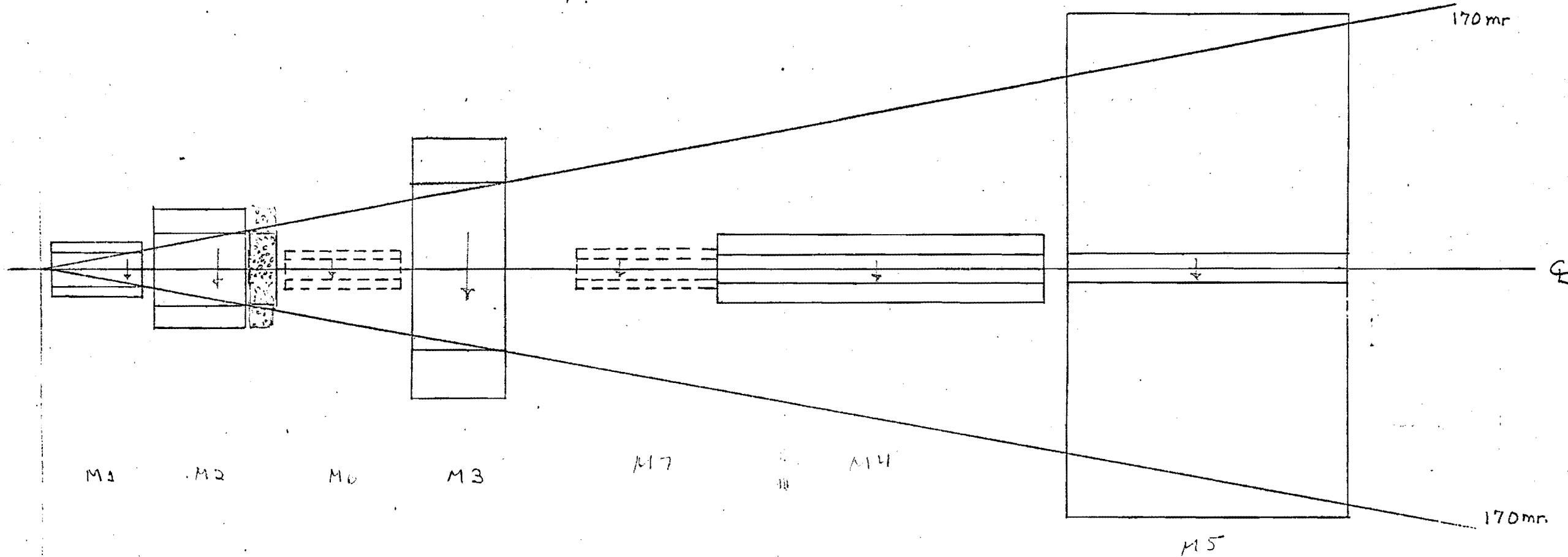
SIDE VIEW

SCALE: 1CM = 1M

ALL FILLS

M3 SUPERCONDUCTING (AL) ...

APPENDIX II

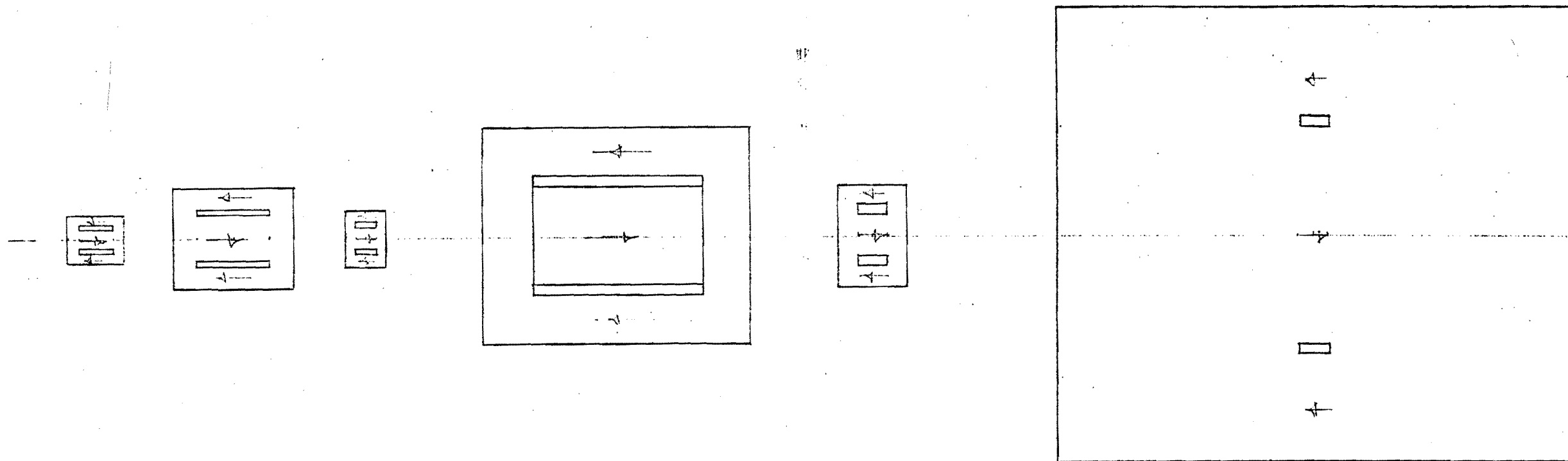


b - TOP VIEW (MID PLANE)

SCALE 1cm = 1m

APPENDIX II

C - MAGNETS (FRONT VIEW)



M1	M2	M6, M7
SIZE(m) .92 x 1.12	2 x 2.42	1.06 x .18
GAP(cm) 8 x 74	8 x 150	12 x 40

M3
4.4 x 5.4
20 x 340

M4
2 x 1.4
20 x 60

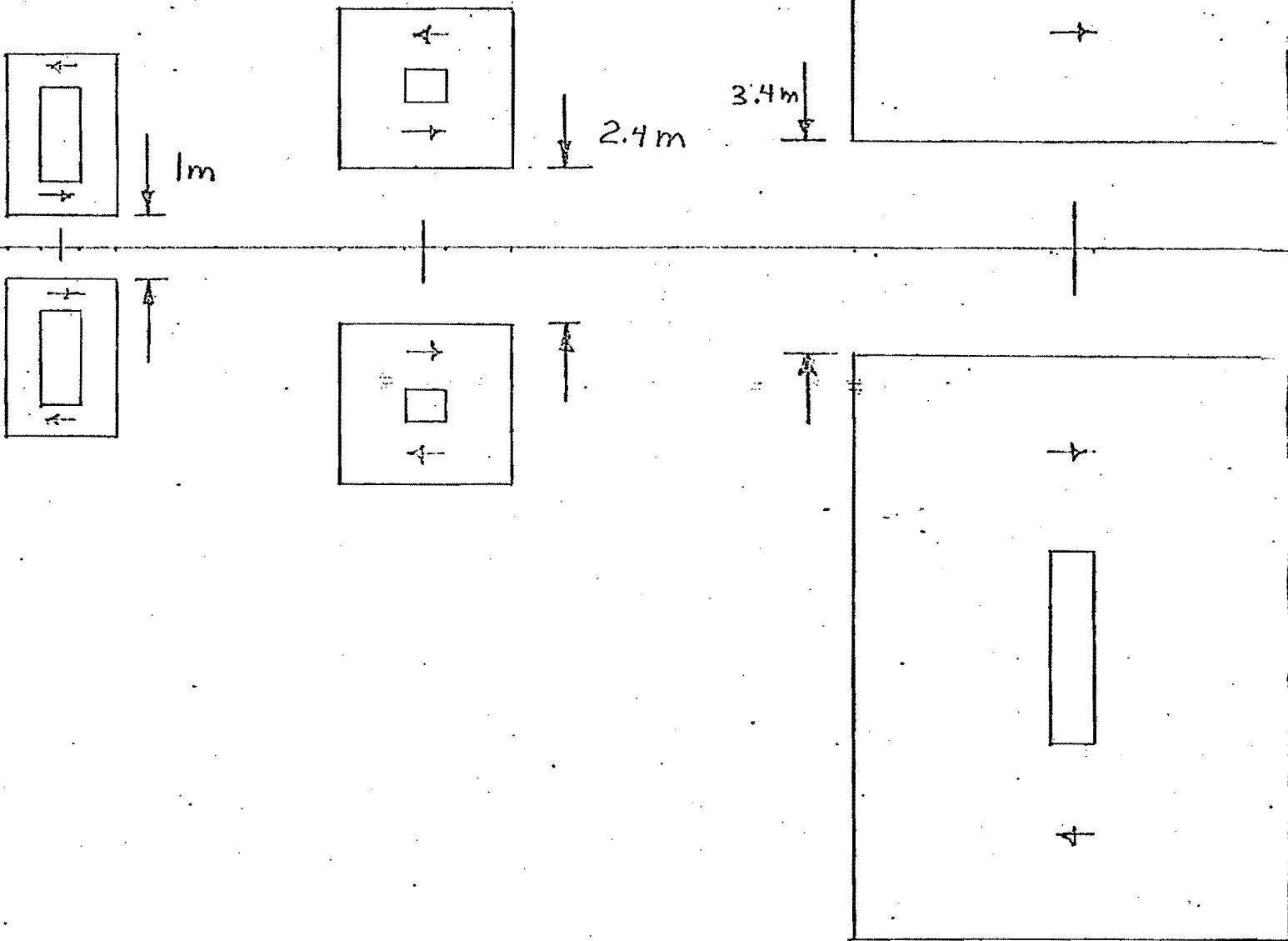
M5
9.2 x 10.4
20 x 60

SCALE : 1CM = 1M

APPENDIX II

d: SPOILERS (FRONT VIEW)

SIZES IN M
GAPS IN CM



S1

SIZE 2,5 x 1,6
GAP: 150 x 60

S2

2,5 x 2,6
50 x 60

S3

9 x 6,6
300 x 60